

Force Dipole Interactions in Membranes with Odd Viscosity

Sneha Krishnan,¹ Udaya Maurya,² and Rickmoy Samanta¹

¹*Birla Institute of Technology and Science, Pilani,*

Hyderabad Campus, Telangana 500078, India

²*Institute for Plasma Research, Bhat, Gandhinagar, India*

We develop a hydrodynamic framework for the interactions and collective dynamics of force dipoles embedded in a compressible fluid membrane supported by a shallow viscous subphase. Starting from the generalized two-dimensional Stokes equations with shear, dilatational, and odd (Hall) viscosities, we derive an exact real-space Green tensor using Hankel transforms. The resulting tensor is characterized by three hydrodynamic screening scales associated with shear, compressional, and odd-viscous modes, and smoothly reduces to the standard limiting cases of incompressible membranes and compressible parity-symmetric membranes, while also capturing the chiral response generated by odd viscosity. Using this Green tensor we obtain the velocity and vorticity fields generated by a force dipole and formulate the dynamical system governing interacting dipoles. The analysis reveals several distinct dynamical regimes and identifies observables that isolate the antisymmetric odd-viscous contribution to dipole interactions, including transverse drift and chiral relative motion.

CONTENTS

I. Introduction	2
II. Basic setup and analytic solution using Hankel transform	7
A. Comments on screening lengths	11
III. Useful limits of the membrane Green tensor, fluid velocity and vorticity	12
A. Compressible limit with vanishing odd viscosity	12
B. Incompressible parity-symmetric limit of the Green tensor	15

C. Degenerate identical-screening limit	18
1. Near Field	20
2. Far field	21
IV. Dynamical system for interacting force dipoles on the membrane	22
A. COM drift and Polarization evolution equations	25
B. Pair Geometry	26
V. Specialization to the two-dipole system	27
VI. Two-dipole dynamics in the near-field degenerate limit	30
VII. Two-dipole dynamics in the far-field degenerate limit	36
VIII. Odd contribution to relative pair motion and identification of odd-sector observables	44
IX. Conclusions	46
X. Acknowledgments	48
XI. Data Availability	48
A. Detailed Simulation Figures	48
B. Real-space Green's function for a compressible membrane with odd viscosity	48
1. Structure of the pole contributions	64
C. Parity structure of the Green tensor	66
References	67

I. INTRODUCTION

At microscopic length scales viscous stresses dominate inertial effects, so the motion of swimmers and membrane-bound motor assemblies is governed by Stokesian low-Reynolds-number hydrodynamics [1, 2]. In this regime the linearity of the Stokes equations allows flow

fields to be represented as superpositions of fundamental singularity solutions. Because freely swimming bodies exert no net force or torque on the surrounding fluid, the leading far-field disturbance is not a Stokeslet but a force dipole, or *stresslet*, which distinguishes extensile (pusher) from contractile (puller) activity. Membrane-bound motor proteins, enzymatic complexes, and cytoskeletal assemblies naturally act as force dipoles, converting chemical energy into mechanical stresses on the surrounding membrane fluid and cytoskeleton [3–7]. Force dipoles therefore provide a minimal hydrodynamic description of interactions between active inclusions.

In unbounded momentum-conserving suspensions, hydrodynamic interactions between such dipoles give rise to a wide range of collective phenomena. Extensile (pusher) dipoles destabilize orientationally ordered states, leading to large-scale hydrodynamic instabilities and chaotic low-Reynolds-number turbulent flows [8–14]. Contractile (puller) dipoles exhibit qualitatively different nonlinear behavior and may instead promote clustering or aggregation depending on parameters and dimensionality [15–20]. When swimmers or active inclusions are confined to interfaces or membranes these interactions are strongly modified by the effectively two-dimensional hydrodynamics of the membrane environment. In such systems momentum is transported within the membrane but also dissipates into the surrounding three-dimensional bulk fluid, leading to characteristic screening lengths and mobility kernels first captured in the Saffman–Delbrück theory and its many extensions [21–27].

Recent theoretical and experimental work has shown that pair interactions of inclusions in membranes depend sensitively on membrane rheology, curvature, and coupling to the surrounding fluid [28–35, 37, 49]. In particular, supported membranes with finite subphase depth exhibit screened hydrodynamic interactions governed by characteristic shear and compressional screening lengths. Despite these advances, a systematic hydrodynamic description of force-dipole interactions in compressible membranes remains relatively unexplored. Membrane compressibility introduces additional longitudinal modes that modify the structure of the mobility kernel and can influence dipole coupling and collective dynamics.

Beyond the conventional parity-symmetric viscous response, two-dimensional fluids can also support an antisymmetric contribution to the stress tensor proportional to the strain rate rotated by the Levi-Civita tensor, characterized by the odd (Hall) viscosity. This term, commonly referred to as *odd viscosity* or Hall viscosity, breaks parity and time-reversal

symmetry and generates transverse momentum transport [41–44]. Odd viscosity has been predicted or observed in a variety of chiral active and quantum fluids and is known to produce circulating flows and chiral responses near boundaries and defects. However, its implications for hydrodynamic interactions between active inclusions in membranes remain only partially understood.

In this work we develop a hydrodynamic framework for force–dipole interactions in supported membranes that incorporates both membrane compressibility and odd viscosity. Starting from the generalized two–dimensional Stokes equation with momentum leakage into the surrounding fluid, we derive the real–space Green tensor of the membrane mobility. The resulting response tensor takes the form

$$G_{ij}(\mathbf{r}) = A_0(r)\delta_{ij} + A_1(r)\hat{r}_i\hat{r}_j + A_2(r)\varepsilon_{ij},$$

where the symmetric kernels A_0 and A_1 describe the conventional dissipative hydrodynamic response while the antisymmetric kernel A_2 encodes the chiral contribution associated with odd viscosity. Observables that isolate this antisymmetric sector therefore provide a natural way to characterize odd–viscous effects in dipolar interactions. The radial kernels are governed by screened hydrodynamic modes determined by the interplay between shear stresses, membrane compressibility, and momentum leakage into the bulk subphase.

Using this Green tensor we derive explicit expressions for the velocity and vorticity fields generated by a force dipole in a compressible membrane. These fields form the basic building blocks for describing interactions between active inclusions. Several limiting regimes of the theory are analyzed, including the parity–symmetric case without odd viscosity, the incompressible membrane limit, and a degenerate regime in which the hydrodynamic screening lengths coincide. In this latter case the Green tensor simplifies and allows compact analytic expressions for the dipolar flow fields. The near–field and far–field structures of the resulting flows are examined in detail in order to characterize how the odd sector of the response modifies the transverse velocity field and the vorticity distribution around active dipoles.

Building on the single–dipole solution, we formulate the dynamical equations governing interacting dipoles in the membrane. The resulting many–body system couples dipole positions and orientations through hydrodynamic interactions mediated by the Green tensor. This formulation yields explicit evolution equations for pair motion as well as for global observables such as center–of–mass drift and the polarization of the dipole ensemble.

ble. Specializing to the two-dipole case leads to a closed dynamical system describing the relative separation and orientation dynamics of dipolar pairs. Within this framework odd viscosity generates chiral relative motion and spiral trajectories that do not arise in the parity-symmetric membrane case.

More broadly, the framework developed here provides a systematic continuum description of active dipoles in compressible chiral membrane fluids. The theory connects microscopic dipolar activity with hydrodynamic observables and establishes a basis for studying collective phenomena in active membrane systems. In forthcoming work [51] we will present more systematic multidipole simulations in compressible membranes with odd viscosity based on the dynamical equations derived in this paper.

Finally, we note that the present work builds on and complements a number of previous studies on membrane hydrodynamics and odd viscosity, including Refs. [26–32, 34–37, 43, 47, 48]. While this manuscript was in preparation a related preprint appeared that also analyzes the hydrodynamic Green’s functions and singularity flows in a compressible supported fluid layer with odd viscosity [50]. The two approaches share a similar physical setup but differ somewhat in formulation. In particular, the present work organizes the hydrodynamic response in terms of three characteristic screening scales associated with shear stresses, compressional modes, and the odd-viscous sector. When the antisymmetric bulk coupling vanishes and the substrate interaction reduces to the conventional Brinkman friction describing momentum leakage into the supporting fluid, the present formulation reduces to the setup in Ref. [50], and the Green tensor obtained here recovers the corresponding solution derived in that work. In addition, beyond the real-space Green tensor, the present work develops the associated force-dipole velocity and vorticity fields, analyzes several limiting regimes including the incompressible case, parity symmetric compressible case and a degenerate odd viscous limit, and formulates the resulting interacting two-dipole and many-dipole dynamical systems.

a. Organization of the paper. The remainder of the paper is organized as follows. In Sec. II we formulate the continuum description of a compressible supported membrane with shear, dilatational, and odd viscosities and obtain the real-space Green tensor of the generalized Stokes operator using a Hankel transform solution. From this tensor we derive the velocity and vorticity fields generated by a force dipole and introduce the three characteristic hydrodynamic screening lengths associated with shear, compressional, and odd-sector

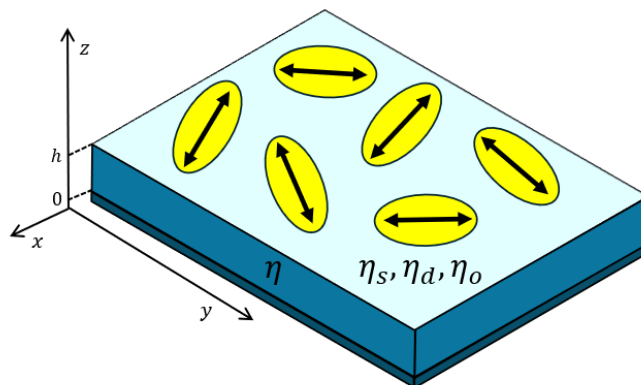


FIG. 1: Schematic illustration of interacting force dipole motors confined to a fluid interface. Each yellow ellipse represents a particle, with the double-headed arrow indicating its orientation. The light blue layer corresponds to a two-dimensional membrane with viscosity η_s, η_d, η_o , supported by a fluid subphase of viscosity η above a rigid substrate.

couplings.

In Sec. III we examine several useful limits of the Green tensor and the dipolar flow fields, including the parity-symmetric compressible case, the incompressible supported membrane limit, and the identical-screening degenerate regime in which the hydrodynamic poles coalesce.

Subsequently we use the dipolar solution to construct the dynamical equations governing interacting active dipoles embedded in the membrane. We derive the general many-dipole dynamical system, analyze global observables such as center-of-mass motion and polarization, and then specialize to the two-dipole problem. Analytical results are presented for both near-field and far-field regimes, including the degenerate screening limit where the pair dynamics admits a compact description and exhibits chiral spiral trajectories.

Finally, we discuss the structure of the odd-viscosity contribution to pair motion and identify observables that isolate the antisymmetric hydrodynamic response. Technical details of the Hankel transform derivation of the real-space Green tensor, the pole structure of the generalized Stokes operator and detailed simulation figures in all regimes are provided in the Appendix.

II. BASIC SETUP AND ANALYTIC SOLUTION USING HANKEL TRANSFORM

Our explorations are based on the setup presented in Fig. 1 in which we model the membrane as a two-dimensional fluid layer with shear viscosity (η_s) and dilatation viscosity (η_d) in the presence of odd viscosity (η_o), on top of a subphase of height h and viscosity η . At the length and time scales relevant for membrane-embedded inclusions, inertial terms are negligible and the membrane velocity is determined by instantaneous balance between viscous stresses and applied forces [1, 2]. We model the membrane as a two-dimensional isotropic fluid layer that supports both shear and dilatational stresses, characterized by a shear viscosity η_s and a dilatation (compressional) viscosity η_d [4, 21, 22]. When microscopic activity breaks time-reversal and parity, the general linear, isotropic constitutive relation admits a nondissipative, antisymmetric contribution known as odd (Hall) viscosity [41–44, 47, 48]. Following Refs. [47, 48], we treat η_o as an effective coarse-grained parameter that captures the macroscopic response of a homogeneously distributed chiral active medium, such as rotor- or torque-generating inclusions embedded in the membrane. In a strictly incompressible membrane ($\eta_d \rightarrow \infty$), the velocity field and Green's function are independent of the odd viscosity, rendering odd-viscous effects hydrodynamically invisible, except via edge modes. Allowing finite compressibility activates longitudinal modes that couple directly to antisymmetric stresses, thereby restoring odd-viscosity contributions to the compressible membrane mobility tensor. The resulting in-plane membrane dynamics are governed by a generalized two-dimensional Stokes equation. In the overdamped regime, instantaneous force balance requires that viscous stresses within the membrane, pressure gradients arising from coupling to the surrounding fluid, and externally applied force densities balance. The membrane velocity field $\mathbf{v}(\mathbf{r})$ thus satisfies

$$\eta_s \nabla^2 \mathbf{v} + \eta_d \nabla (\nabla \cdot \mathbf{v}) + \eta_o \nabla^2 \mathbf{v}^* - \frac{h}{2} \nabla p + \mathbf{f}^{3D} + \mathbf{F} = \mathbf{0}, \quad (1)$$

where $\mathbf{v}_i^* = \varepsilon_{ij} v_j$ denotes the velocity rotated by $\pi/2$, p is the pressure field in the underlying three-dimensional fluid, \mathbf{f}^{3D} represents momentum exchange between the membrane and its environment, and \mathbf{F} is the in-plane force density generated by embedded inclusions, such as that generated by membrane-anchored force dipoles. The first two terms describe dissipative shear and dilatational stresses, while the third term, proportional to the odd viscosity η_o , is antisymmetric and nondissipative, encoding a transverse stress response that breaks parity

and time-reversal symmetry. Coupling to the bulk fluid leads to momentum leakage, which we model as [24] Brinkman-like friction coefficients ζ_{\parallel} and ζ_{\perp}

$$f_i^{3D} = -(\zeta_{\parallel} \delta_{ij} + \zeta_{\perp} \epsilon_{ij}) v_j. \quad (2)$$

In the presence of a *shallow* subphase, the longitudinal coupling can be well approximated [26] as

$$\zeta_{\parallel} \sim \frac{\eta}{h}, \quad (3)$$

For completeness, we note that in the limit of an unsupported (free) membrane, the longitudinal friction coefficient $\zeta_{\parallel}(q)$ is in general *linear* in the in-plane wavenumber q , reflecting the well-known Saffman–Delbrück momentum leakage into a semi-infinite fluid. Since this introduces qualitatively distinct hydrodynamic behavior, we do not consider the unsupported-membrane limit in this work and defer a detailed analysis to a future communication.

The force balance equation is closed by a compressibility relation obtained under the lubrication approximation [47, 48],

$$\nabla \cdot \mathbf{v} = \frac{h^2}{6\eta} \nabla^2 p. \quad (4)$$

where η is the bulk fluid shear viscosity and h is the subphase depth. In the lubrication limit, appropriate for a shallow subphase where h is small compared to lateral hydrodynamic length scales, the three-dimensional Stokes equation in the subphase can be solved explicitly with no-slip boundary conditions at the substrate and velocity continuity at the membrane interface [45, 47]. Taking the divergence of the bulk flow and integrating across the subphase thickness $0 \leq z \leq h$ yields the closure relation Eq. (4) linking the in-plane compressibility of the membrane flow to pressure variations in the subphase. More complex situations involving surfactant-mediated interfacial stresses and additional hidden dynamical variables can further modify this coupling mechanism [46]; however, for analytical tractability we restrict our attention here to the lubrication regime. Together, Eqs. (1) and (4) provide a minimal continuum description of a compressible supported membrane with shear and odd viscosities, capturing conventional dissipative in-plane momentum transport, screening due to bulk momentum leakage, and nondissipative chiral transport arising from the breaking of time-reversal and parity symmetries [47, 48].

Because the Stokes operator defined by Eqs. (1) is linear and translationally invariant in the membrane plane, the velocity generated by any localized forcing can be written in

terms of the associated Green's tensor $G_{ij}(\mathbf{r})$. For force-free active inclusions, the monopole (Stokeslet) contribution vanishes, and the leading term in the multipole expansion is the force dipole (stresslet). Differentiating the Stokeslet along the dipole axis then yields the dipolar flow, taking the form,

$$v_i(\mathbf{r}) = \sigma \hat{d}_k \partial_k G_{ij}(\mathbf{r}) \hat{d}_j, \quad (5)$$

where $\hat{\mathbf{d}}$ denotes the dipole orientation and $\sigma \equiv \text{FL}$ is the dipole strength, with L the dipole size ($\sigma > 0$ for pushers and $\sigma < 0$ for pullers). The full Green's function for a Stokeslet point force \mathbf{F} in this system is given by (see Appendix B for a detailed derivation using Hankel transforms),

$$G_{ij}(\mathbf{r}) = A_0(r) \delta_{ij} + A_1(r) \hat{r}_i \hat{r}_j + A_2(r) \varepsilon_{ij}, \quad r = |\mathbf{r}|, \quad \hat{r}_i = r_i/r, \quad (6)$$

where

$$\begin{aligned} A_0(r) &= \frac{1}{2\pi} \sum_{i=1}^2 R_i^{(\beta)} K_0(m_i r) + \frac{C_0}{2\pi} \frac{1}{r^2} + \frac{1}{2\pi} \sum_{i=1}^2 C_i \frac{m_i K_1(m_i r)}{r} \\ A_1(r) &= -\frac{1}{2\pi} \sum_{i=1}^2 C_i m_i^2 K_0(m_i r) - \frac{1}{\pi} \sum_{i=1}^2 C_i \frac{m_i K_1(m_i r)}{r} - \frac{C_0}{\pi} \frac{1}{r^2} \\ A_2(r) &= \frac{1}{2\pi} \sum_{i=1}^2 R_i^{(\gamma)} K_0(m_i r) \end{aligned} \quad (7)$$

where K_0, K_1 are modified Bessel functions of the second kind. The method to compute the coefficients m_1, m_2, C_i and the residues $R^{(\beta)}, R^{(\gamma)}$, is provided explicitly below. We first define

$$\begin{aligned} A &= \eta_s(\eta_s + \eta_d) + \eta_o^2, \\ B &= \eta_s(\eta_s + \eta_d)(\kappa^2 + \lambda^2) + 2\eta_o^2 \nu^2, \\ C &= \eta_s(\eta_s + \eta_d)\kappa^2 \lambda^2 + \eta_o^2 \nu^4. \end{aligned}$$

where the hydrodynamic screening lengths are defined as

$$\kappa^{-1} = \sqrt{\frac{\eta_s}{\zeta_{\parallel}}}, \quad \lambda^{-1} = \sqrt{\frac{h(\eta_s + \eta_d)}{3\eta + h\zeta_{\parallel}}}, \quad \nu^{-1} = \sqrt{\frac{\eta_o}{\zeta_{\perp}}}. \quad (8)$$

This helps us construct Δ

$$\Delta = B^2 - 4AC,$$

and importantly, the two *screening masses*, named in analogy with Yukawa interactions,

$$m_1 = \sqrt{\frac{B - \sqrt{\Delta}}{2A}}, \quad m_2 = \sqrt{\frac{B + \sqrt{\Delta}}{2A}}.$$

The $R^{(\beta)}$ and $R^{(\gamma)}$ residues are given by

$$R_1^{(\beta)} = \frac{(\eta_s + \eta_d)}{\sqrt{\Delta}} \left(\frac{-B + \sqrt{\Delta}}{2A} + \lambda^2 \right) = \frac{\eta_s + \eta_d}{2A\sqrt{\Delta}} (-B + \sqrt{\Delta} + 2A\lambda^2),$$

$$R_2^{(\beta)} = -\frac{(\eta_s + \eta_d)}{\sqrt{\Delta}} \left(\frac{-B - \sqrt{\Delta}}{2A} + \lambda^2 \right) = -\frac{\eta_s + \eta_d}{2A\sqrt{\Delta}} (-B - \sqrt{\Delta} + 2A\lambda^2),$$

$$R_1^{(\gamma)} = -\frac{\eta_o}{\sqrt{\Delta}} \left(\frac{-B + \sqrt{\Delta}}{2A} + \nu^2 \right) = -\frac{\eta_o}{2A\sqrt{\Delta}} (-B + \sqrt{\Delta} + 2A\nu^2),$$

$$R_2^{(\gamma)} = \frac{\eta_o}{\sqrt{\Delta}} \left(\frac{-B - \sqrt{\Delta}}{2A} + \nu^2 \right) = \frac{\eta_o}{2A\sqrt{\Delta}} (-B - \sqrt{\Delta} + 2A\nu^2).$$

The coefficients C_0, C_1, C_2 are given by

$$C_0 = \frac{\eta_s \kappa^2 - (\eta_s + \eta_d)\lambda^2}{C}.$$

$$C_1 = \frac{-\eta_d(-B + \sqrt{\Delta}) + 2AN_0}{(-B + \sqrt{\Delta})\sqrt{\Delta}},$$

$$C_2 = \frac{\eta_d(B + \sqrt{\Delta}) + 2AN_0}{(B + \sqrt{\Delta})\sqrt{\Delta}}.$$

where $N_0 = \eta_s \kappa^2 - (\eta_s + \eta_d)\lambda^2$. The velocity field generated by a force dipole of strength σ and orientation $\hat{\mathbf{d}}$ takes the form

$$\mathbf{v}(\mathbf{r}) = \sigma \left[\alpha \left(A_0'(r) + \frac{A_1(r)}{r} \right) \hat{\mathbf{d}} + \left(\frac{A_1(r)}{r} + \alpha^2 \left(A_1'(r) - \frac{2A_1(r)}{r} \right) \right) \hat{\mathbf{r}} + \alpha A_2'(r) (\boldsymbol{\varepsilon} \cdot \hat{\mathbf{d}}) \right], \quad (9)$$

while the associated vorticity field is

$$\boldsymbol{\omega}(\mathbf{r}) = \sigma \left[\alpha \beta \left(A_0''(r) - \frac{A_0'(r)}{r} - \frac{A_1'(r)}{r} + \frac{2A_1(r)}{r^2} \right) - \left(\frac{A_2'(r)}{r} \beta^2 + \alpha^2 A_2''(r) \right) \right]. \quad (10)$$

These expressions provide the complete hydrodynamic velocity and vorticity fields generated by a force dipole in the membrane once the radial Green tensor functions $A_0(r)$, $A_1(r)$ and $A_2(r)$ are specified. The geometry of the flow relative to the dipole orientation is conveniently described using the scalars

$$\alpha = d_i \hat{r}_i, \quad (11)$$

and

$$\beta = \varepsilon_{ij} d_j \hat{r}_i, \quad (12)$$

which represent the projections of the dipole orientation along the radial and transverse directions, respectively. Because the dipole orientation vector \mathbf{d} is normalized, these scalars satisfy

$$\alpha^2 + \beta^2 = 1. \quad (13)$$

Together, Eqs. (11)-(12) provide a compact parameterization of the relative orientation between the dipole axis and the observation direction $\hat{\mathbf{r}}$, allowing the dipolar flow and vorticity fields to be expressed entirely in terms of the scalar functions $A_0(r)$, $A_1(r)$ and $A_2(r)$ and their radial derivatives.

A. Comments on screening lengths

The three screening lengths in Eq. (8) set the spatial range of distinct hydrodynamic modes in a supported membrane and delimit crossovers between qualitatively different flow regimes. The shear screening length $\kappa^{-1} = \sqrt{\eta_s/\zeta_{\parallel}}$ controls shear modes: for $r \ll \kappa^{-1}$ the flow resembles unscreened 2D Stokes hydrodynamics, while for $r \gg \kappa^{-1}$ shear disturbances are suppressed by momentum leakage into the subphase. The compressional length $\lambda^{-1} = \sqrt{h(\eta_s + \eta_d)/(3\eta + h\zeta_{\parallel})}$ governs longitudinal (dilation/compression) modes, reflecting the competition between membrane compressibility and pressure-driven drainage in the underlying 3D fluid. The odd-viscous length $\nu^{-1} = \sqrt{\eta_o/\zeta_{\perp}}$ sets the range of chiral, Hall-like momentum transport that appears only when both parity and time-reversal symmetries are broken; this channel is nondissipative and produces transverse, lift-like responses without entropy production.

In the shallow-subphase (Brinkman) approximation one has $\zeta_{\parallel} \sim \eta/h$ and often ζ_{\perp} is approximated as [47, 48]

$$\zeta_{\perp} \sim \left(\frac{\eta_o}{\eta_s}\right) \zeta_{\parallel} \equiv \mu \zeta_{\parallel}. \quad (14)$$

so that $\mu = \eta_o/\eta_s$ is a dimensionless measure of odd-to-shear response. In this limit μ links ν^{-1} to κ^{-1} ; relaxing this proportionality makes ν^{-1} an independent crossover scale and allows odd-viscous transport to dominate at intermediate distances even when conventional shear is strongly screened. We will not use the approximation of Eq. (14) except while specializing to a degenerate limit in Sec. III C.

III. USEFUL LIMITS OF THE MEMBRANE GREEN TENSOR, FLUID VELOCITY AND VORTICITY

We now record several limiting cases of the general Green tensor derived above. These limits provide useful checks for the full Green tensor presented here and clarify how the general solution reduces to familiar parity-symmetric membrane hydrodynamics when the odd viscosity vanishes, as well as how it simplifies in the identical-screening degenerate regime.

A. Compressible limit with vanishing odd viscosity

It is useful to verify that the general Green tensor derived above reduces to the standard compressible membrane mobility when odd viscosity is switched off. This provides a nontrivial consistency check of the analytic solution obtained from the Hankel transform.

We therefore consider the limit

$$\eta_o \rightarrow 0.$$

In this case the antisymmetric stresses vanish and the hydrodynamics becomes parity symmetric. The characteristic coefficients introduced in the general solution simplify considerably. From the definitions

$$A = \eta_s(\eta_s + \eta_d) + \eta_o^2, \quad B = \eta_s(\eta_s + \eta_d)(\kappa^2 + \lambda^2) + 2\eta_o^2\nu^2, \quad C = \eta_s(\eta_s + \eta_d)\kappa^2\lambda^2 + \eta_o^2\nu^4,$$

we obtain

$$A = \eta_s(\eta_s + \eta_d),$$

$$B = \eta_s(\eta_s + \eta_d)(\kappa^2 + \lambda^2),$$

$$C = \eta_s(\eta_s + \eta_d)\kappa^2\lambda^2.$$

The discriminant entering the pole structure becomes

$$\Delta = B^2 - 4AC = [\eta_s(\eta_s + \eta_d)]^2(\kappa^2 - \lambda^2)^2.$$

Consequently

$$\sqrt{\Delta} = \eta_s(\eta_s + \eta_d) |\kappa^2 - \lambda^2|.$$

Substituting these expressions into the definitions of the screening masses

$$m_{1,2}^2 = \frac{B \mp \sqrt{\Delta}}{2A},$$

we find that the two poles reduce to the physical shear and compressional screening scales,

$$m_1^2 = \lambda^2, \quad m_2^2 = \kappa^2,$$

up to a trivial relabeling of the indices depending on the relative magnitude of κ and λ .

The residues appearing in the Green tensor also simplify. The antisymmetric residues are proportional to η_o and therefore vanish identically,

$$R_1^{(\gamma)} = R_2^{(\gamma)} = 0.$$

As a result the antisymmetric kernel disappears,

$$A_2(r) = 0.$$

The symmetric residues become

$$R_1^{(\beta)} = 0, \quad R_2^{(\beta)} = \frac{1}{\eta_s}.$$

The coefficients entering the algebraic part of the Green tensor are

$$C_0 = \frac{\eta_s \kappa^2 - (\eta_s + \eta_d) \lambda^2}{\eta_s (\eta_s + \eta_d) \kappa^2 \lambda^2} = \frac{1}{(\eta_s + \eta_d) \lambda^2} - \frac{1}{\eta_s \kappa^2},$$

$$C_1 = -\frac{1}{(\eta_s + \eta_d) \lambda^2}, \quad C_2 = \frac{1}{\eta_s \kappa^2}.$$

Substituting these simplified coefficients into the general expressions for the radial Green tensor functions yields

$$A_0(r) = \frac{1}{2\pi} \left[\frac{1}{\eta_s} \left(K_0(\kappa r) + \frac{K_1(\kappa r)}{\kappa r} - \frac{1}{(\kappa r)^2} \right) - \frac{1}{\eta_s + \eta_d} \left(\frac{K_1(\lambda r)}{\lambda r} - \frac{1}{(\lambda r)^2} \right) \right],$$

$$A_1(r) = \frac{1}{2\pi} \left[\frac{1}{\eta_s + \eta_d} \left(K_0(\lambda r) + \frac{2K_1(\lambda r)}{\lambda r} - \frac{2}{(\lambda r)^2} \right) - \frac{1}{\eta_s} \left(K_0(\kappa r) + \frac{2K_1(\kappa r)}{\kappa r} - \frac{2}{(\kappa r)^2} \right) \right].$$

The antisymmetric coefficient vanishes,

$$A_2(r) = 0.$$

The real-space Green tensor therefore reduces to

$$G_{ij}(\mathbf{r}) = A_0(r)\delta_{ij} + A_1(r)\hat{r}_i\hat{r}_j.$$

This expression is the Green function for a compressible supported membrane without odd viscosity. The hydrodynamic response separates into two screened channels corresponding to transverse shear and longitudinal compression. The shear sector is screened over the length scale κ^{-1} , while the compressional sector is screened over the length scale λ^{-1} . In contrast to the general case with odd viscosity, no antisymmetric component proportional to ε_{ij} survives, reflecting the restoration of parity symmetry in the membrane dynamics. In this case it is useful to write the Green tensor in the Helmholtz form

$$G_{ij}(\mathbf{r}) = G_L(r)\hat{r}_i\hat{r}_j + G_T(r)(\delta_{ij} - \hat{r}_i\hat{r}_j), \quad (15)$$

with

$$G_L(r) = \frac{1}{2\pi} \left\{ \frac{1}{\eta_s + \eta_d} \left[K_0(\lambda r) + \frac{K_1(\lambda r)}{\lambda r} - \frac{1}{\lambda^2 r^2} \right] + \frac{1}{\eta_s} \left[\frac{1}{\kappa^2 r^2} - \frac{K_1(\kappa r)}{\kappa r} \right] \right\}, \quad (16)$$

$$G_T(r) = \frac{1}{2\pi} \left\{ \frac{1}{\eta_s + \eta_d} \left[\frac{1}{\lambda^2 r^2} - \frac{K_1(\lambda r)}{\lambda r} \right] + \frac{1}{\eta_s} \left[K_0(\kappa r) + \frac{K_1(\kappa r)}{\kappa r} - \frac{1}{\kappa^2 r^2} \right] \right\}. \quad (17)$$

The corresponding force-dipole velocity and vorticity fields then follow directly from the general formulas derived in the previous section. The incompressible result is recovered smoothly in the limit $\eta_d \rightarrow \infty$, for which the longitudinal mode is suppressed. In the compressible parity-symmetric case with vanishing odd viscosity ($\eta_o = 0$), the antisymmetric Green-tensor component vanishes, $A_2(r) = 0$, and the dipole velocity field follows from Eq. (9) after substituting the compressible Green-tensor coefficients $A_0(r)$ and $A_1(r)$. The resulting flow can be written in the compact form

$$\mathbf{v}(\mathbf{r}) = \sigma \left[\alpha C_d(r) \hat{\mathbf{d}} + C_r(r) \hat{\mathbf{r}} \right], \quad (18)$$

where $\alpha = \hat{\mathbf{d}} \cdot \hat{\mathbf{r}}$. The radial coefficients receive independent contributions from the shear (κ) and compressional (λ) hydrodynamic modes and are given by

$$C_d(r) = \frac{1}{2\pi} \left[\frac{1}{\eta_s} \left(-\kappa K_1(\kappa r) - \frac{2K_2(\kappa r)}{r} + \frac{4}{\kappa^2 r^3} \right) + \frac{1}{\eta_s + \eta_d} \left(\frac{2K_2(\lambda r)}{r} - \frac{4}{\lambda^2 r^3} \right) \right]. \quad (19)$$

$$C_r(r) = \frac{1}{2\pi} \left[\frac{1}{\eta_s} \left(\alpha^2 \kappa K_1(\kappa r) + \frac{(4\alpha^2 - 1)K_2(\kappa r)}{r} + \frac{2 - 8\alpha^2}{\kappa^2 r^3} \right) - \frac{1}{\eta_s + \eta_d} \left(\alpha^2 \lambda K_1(\lambda r) + \frac{(4\alpha^2 - 1)K_2(\lambda r)}{r} + \frac{2 - 8\alpha^2}{\lambda^2 r^3} \right) \right]. \quad (20)$$

Here $\kappa^{-1} = \sqrt{\eta_s/\zeta_{\parallel}}$ is the shear screening length, and $\lambda^{-1} = \sqrt{(\eta_s + \eta_d)/\zeta_{\parallel}}$ is the compressional screening length. In the incompressible limit $\eta_d \rightarrow \infty$, the compressional contribution vanishes and the velocity reduces smoothly to the incompressible dipole flow obtained in the previous section. The vorticity field follows from Eq. (10). For the parity-symmetric case with vanishing odd viscosity ($\eta_o = 0$) the antisymmetric Green tensor component vanishes, $A_2(r) = 0$, and the vorticity reduces to

$$\omega(\mathbf{r}) = \sigma \alpha \beta \left(A_0''(r) - \frac{A_0'(r)}{r} - \frac{A_1'(r)}{r} + \frac{2A_1(r)}{r^2} \right). \quad (21)$$

Substituting the compressible Green tensor coefficients $A_0(r)$ and $A_1(r)$ and simplifying yields the remarkably simple result

$$\omega(\mathbf{r}) = \frac{\sigma}{2\pi\eta_s} \alpha \beta \kappa^2 K_2(\kappa r). \quad (22)$$

Thus the compressional hydrodynamic mode does not contribute to the dipolar vorticity; it produces only irrotational (longitudinal) flow. The vorticity is therefore identical to the incompressible supported-membrane result.

B. Incompressible parity-symmetric limit of the Green tensor

It is useful to examine the limit in which both odd viscosity and membrane compressibility are removed. This corresponds to taking

$$\eta_o \rightarrow 0, \quad \eta_d \rightarrow \infty.$$

In this regime the antisymmetric stresses vanish and the membrane flow becomes incompressible. The resulting Green tensor therefore provides a useful consistency check of the general solution derived above.

We begin from the definitions of the coefficients appearing in the general solution,

$$A = \eta_s(\eta_s + \eta_d) + \eta_o^2, \quad B = \eta_s(\eta_s + \eta_d)(\kappa^2 + \lambda^2) + 2\eta_o^2\nu^2, \quad C = \eta_s(\eta_s + \eta_d)\kappa^2\lambda^2 + \eta_o^2\nu^4.$$

Taking the parity-symmetric limit $\eta_o \rightarrow 0$ gives

$$A = \eta_s(\eta_s + \eta_d), \quad B = \eta_s(\eta_s + \eta_d)(\kappa^2 + \lambda^2), \quad C = \eta_s(\eta_s + \eta_d)\kappa^2\lambda^2.$$

The hydrodynamic screening lengths are defined by

$$\kappa^{-1} = \sqrt{\frac{\eta_s}{\zeta_{\parallel}}}, \quad \lambda^{-1} = \sqrt{\frac{h(\eta_s + \eta_d)}{3\eta + h\zeta_{\parallel}}}.$$

In the incompressible limit $\eta_d \rightarrow \infty$ the longitudinal screening length diverges,

$$\lambda^{-1} \rightarrow \infty, \quad \lambda \rightarrow 0.$$

The discriminant entering the pole structure of the Green tensor is

$$\Delta = B^2 - 4AC.$$

Substituting the simplified coefficients gives

$$\Delta = [\eta_s(\eta_s + \eta_d)]^2\kappa^4.$$

Consequently

$$\sqrt{\Delta} = \eta_s(\eta_s + \eta_d)\kappa^2.$$

The screening masses defined by

$$m_{1,2}^2 = \frac{B \mp \sqrt{\Delta}}{2A}$$

then reduce to

$$m_1^2 = 0, \quad m_2^2 = \kappa^2.$$

Thus the hydrodynamics contains a massless incompressible mode together with a single screened shear mode characterized by the screening length κ^{-1} .

The residues appearing in the antisymmetric sector are proportional to η_o and therefore vanish,

$$R_1^{(\gamma)} = R_2^{(\gamma)} = 0.$$

As a result the antisymmetric Green tensor component disappears,

$$A_2(r) = 0.$$

The symmetric residues become

$$R_1^{(\beta)} = 0, \quad R_2^{(\beta)} = \frac{1}{\eta_s}.$$

Substituting these results into the general expressions for the radial functions yields

$$A_0(r) = \frac{1}{2\pi\eta_s} \left[K_0(\kappa r) + \frac{K_1(\kappa r)}{\kappa r} - \frac{1}{(\kappa r)^2} \right],$$

$$A_1(r) = -\frac{1}{2\pi\eta_s} \left[K_0(\kappa r) + \frac{2K_1(\kappa r)}{\kappa r} - \frac{2}{(\kappa r)^2} \right].$$

The antisymmetric coefficient vanishes,

$$A_2(r) = 0.$$

The Green tensor therefore reduces to the purely symmetric form

$$G_{ij}(\mathbf{r}) = A_0(r)\delta_{ij} + A_1(r)\hat{r}_i\hat{r}_j, \quad r = |\mathbf{r}|.$$

This expression represents the velocity response of an incompressible supported membrane with momentum leakage to the surrounding fluid. The hydrodynamic flow is screened over the characteristic length scale κ^{-1} and contains only transverse shear modes, reflecting both the incompressibility of the membrane and the restoration of parity symmetry when odd viscosity is removed. Substituting the incompressible Green-tensor coefficients into the general dipolar velocity expression yields the force-dipole flow in the compact form

$$\mathbf{v}(\mathbf{r}) = \sigma \left[\alpha C_d(r) \hat{\mathbf{d}} + C_r(r) \hat{\mathbf{r}} \right], \quad (23)$$

where $\alpha = \hat{\mathbf{d}} \cdot \hat{\mathbf{r}}$ and the radial coefficients are

$$C_d(r) = \frac{1}{2\pi\eta_s} \left[-\kappa K_1(\kappa r) - \frac{2K_2(\kappa r)}{r} + \frac{4}{\kappa^2 r^3} \right], \quad (24)$$

$$C_r(r) = \frac{1}{2\pi\eta_s} \left[\alpha^2 \kappa K_1(\kappa r) + \frac{(4\alpha^2 - 1)K_2(\kappa r)}{r} + \frac{2 - 8\alpha^2}{\kappa^2 r^3} \right]. \quad (25)$$

The incompressible dipole velocity therefore depends only on the screened kernels K_1 and K_2 , while the transverse odd-viscous contribution vanishes identically in this limit. In polar it reads

$$v_r(\mathbf{r}) = \frac{\sigma}{2\pi\eta_s} (2\alpha^2 - 1) \left[\frac{K_2(\kappa r)}{r} - \frac{2}{\kappa^2 r^3} \right], \quad (26)$$

$$v_\theta(\mathbf{r}) = \frac{\sigma \alpha \beta}{2\pi\eta_s} \left[-\kappa K_1(\kappa r) - \frac{2K_2(\kappa r)}{r} + \frac{4}{\kappa^2 r^3} \right], \quad (27)$$

where $r = |\mathbf{r}|$, $\kappa^{-1} = \sqrt{\eta_s h / \eta}$ is the hydrodynamic screening length, Since $A_2 = 0$, the vorticity reduces to

$$\omega(\mathbf{r}) = \sigma \alpha \beta \left(A_0''(r) - \frac{A_0'(r)}{r} - \frac{A_1'(r)}{r} + \frac{2A_1(r)}{r^2} \right), \quad (28)$$

which simplifies to the compact form

$$\omega(\mathbf{r}) = \frac{\sigma}{2\pi\eta_s} \alpha \beta \kappa^2 K_2(\kappa r). \quad (29)$$

Thus, in the incompressible supported-membrane limit, the dipolar vorticity is controlled entirely by the screened kernel $K_2(\kappa r)$.

C. Degenerate identical-screening limit

Finally, we consider the identical-screening degenerate limit of the full compressible odd-viscous theory. Starting from the general solution with screening masses

$$m_{1,2}^2 = \frac{B \mp \sqrt{\Delta}}{2A}, \quad \Delta = B^2 - 4AC,$$

where

$$\begin{aligned} A &= \eta_s(\eta_s + \eta_d) + \eta_o^2, \\ B &= \eta_s(\eta_s + \eta_d)(\kappa^2 + \lambda^2) + 2\eta_o^2\nu^2, \\ C &= \eta_s(\eta_s + \eta_d)\kappa^2\lambda^2 + \eta_o^2\nu^4, \end{aligned}$$

we impose

$$\zeta_{\parallel} = \frac{\eta}{h}, \quad \eta_d = 3\eta_s, \quad \zeta_{\perp} = \frac{\eta_o}{\eta_s} \zeta_{\parallel}. \quad (30)$$

The three screening lengths then coincide,

$$\kappa = \lambda = \nu = m, \quad m = \frac{1}{\ell}, \quad \ell = \sqrt{\frac{\eta_s h}{\eta}}, \quad (31)$$

and, since $\eta_s + \eta_d = 4\eta_s$,

$$A = 4\eta_s^2 + \eta_o^2, \quad B = 2Am^2, \quad C = Am^4.$$

Hence

$$\Delta = 0, \quad m_1 = m_2 = m, \quad (32)$$

so the two screening poles coalesce into a single mode. In this limit the Green tensor retains the form

$$G_{ij}(\mathbf{r}) = A_0(r) \delta_{ij} + A_1(r) \hat{r}_i \hat{r}_j + A_2(r) \varepsilon_{ij},$$

but the radial functions collapse to

$$\begin{aligned} A_0(r) &= \frac{\eta_s}{2\pi(4\eta_s^2 + \eta_o^2)} \left[4K_0(mr) - \frac{3}{m^2 r^2} + \frac{3}{mr} K_1(mr) \right], \\ A_1(r) &= \frac{\eta_s}{2\pi(4\eta_s^2 + \eta_o^2)} \left[-3K_0(mr) - \frac{6}{mr} K_1(mr) + \frac{6}{m^2 r^2} \right], \\ A_2(r) &= -\frac{\eta_o}{2\pi(4\eta_s^2 + \eta_o^2)} K_0(mr). \end{aligned} \quad (33)$$

Thus the general two-mode Green tensor reduces to a single-screening form controlled by the length scale ℓ . The odd viscosity enters through the antisymmetric coefficient $A_2(r)$ and through the overall normalization factor $4\eta_s^2 + \eta_o^2$. Substituting these expressions into the general dipole velocity formula

$$\mathbf{v}(\mathbf{r}) = \sigma \left[\alpha \left(A'_0(r) + \frac{A_1(r)}{r} \right) \hat{\mathbf{d}} + \left(\frac{A_1(r)}{r} + \alpha^2 \left(A'_1(r) - \frac{2A_1(r)}{r} \right) \right) \hat{\mathbf{r}} + \alpha A'_2(r) (\boldsymbol{\varepsilon} \cdot \hat{\mathbf{d}}) \right], \quad (34)$$

we obtain the compact form

$$\mathbf{v}(\mathbf{r}) = \sigma \left[\alpha C_d(r) \hat{\mathbf{d}} + C_r(r) \hat{\mathbf{r}} + \alpha C_\perp(r) (\boldsymbol{\varepsilon} \cdot \hat{\mathbf{d}}) \right]. \quad (35)$$

The radial coefficients are

$$\begin{aligned} C_d(r) &= \frac{\eta_s}{\pi(4\eta_s^2 + \eta_o^2)} \left[-\frac{3K_2(mr)}{r} - 2mK_1(mr) + \frac{6}{m^2 r^3} \right], \\ C_r(r) &= \frac{3\eta_s}{2\pi(4\eta_s^2 + \eta_o^2)} \left[\alpha^2 m K_1(mr) + \frac{(4\alpha^2 - 1)K_2(mr)}{r} + \frac{2 - 8\alpha^2}{m^2 r^3} \right], \\ C_\perp(r) &= \frac{m\eta_o}{2\pi(4\eta_s^2 + \eta_o^2)} K_1(mr). \end{aligned}$$

The transverse coefficient C_\perp arises entirely from the antisymmetric Green tensor component and therefore vanishes in the absence of odd viscosity. The vorticity follows from the general expression

$$\boldsymbol{\omega}(\mathbf{r}) = \sigma \left[\alpha\beta \left(A''_0 - \frac{A'_0}{r} - \frac{A'_1}{r} + \frac{2A_1}{r^2} \right) - \left(\frac{A'_2}{r} \beta^2 + \alpha^2 A''_2 \right) \right],$$

which yields

$$\boldsymbol{\omega}(\mathbf{r}) = \frac{\sigma}{2\pi(4\eta_s^2 + \eta_o^2)} \left[4\eta_s \alpha\beta m^2 K_2(mr) + \eta_o \left(\alpha^2 m^2 K_0(mr) + \frac{(2\alpha^2 - 1)m}{r} K_1(mr) \right) \right].$$

Thus the vorticity naturally separates into even- and odd-viscosity contributions,

$$\omega = \omega_{\text{even}} + \omega_{\text{odd}},$$

with

$$\begin{aligned} \omega_{\text{even}}(\mathbf{r}) &= \frac{4\sigma\eta_s}{2\pi(4\eta_s^2 + \eta_o^2)} \alpha\beta m^2 K_2(mr), \\ \omega_{\text{odd}}(\mathbf{r}) &= \frac{\sigma\eta_o}{2\pi(4\eta_s^2 + \eta_o^2)} \left[\alpha^2 m^2 K_0(mr) + \frac{(2\alpha^2 - 1)m}{r} K_1(mr) \right]. \end{aligned} \quad (36)$$

In the limit $\eta_o \rightarrow 0$ the transverse velocity disappears and the vorticity reduces to the purely even-viscosity dipolar form.

1. Near Field

We now examine the near-field behavior of the degenerate Green tensor. In the regime

$$mr \ll 1,$$

corresponding to distances much smaller than the common screening length $\ell = 1/m$, the modified Bessel functions admit the expansions

$$K_0(mr) = -\ln\left(\frac{mr}{2}\right) - \gamma + \mathcal{O}(r^2 \ln r), \quad K_1(mr) = \frac{1}{mr} + \mathcal{O}(r \ln r).$$

Substituting these expressions into the degenerate coefficients $A_0(r)$, $A_1(r)$, and $A_2(r)$, one finds that the explicit $1/r^2$ singularities appearing in A_0 and A_1 cancel. The leading near-field behavior therefore reduces to

$$A_0(r) \simeq -\frac{5\eta_s}{4\pi(4\eta_s^2 + \eta_o^2)} \ln(mr) + \mathcal{O}(1), \quad (37)$$

$$A_1(r) \simeq \frac{3\eta_s}{4\pi(4\eta_s^2 + \eta_o^2)} + \mathcal{O}(r^2 \ln r), \quad (38)$$

$$A_2(r) \simeq \frac{\eta_o}{2\pi(4\eta_s^2 + \eta_o^2)} \ln(mr) + \mathcal{O}(1). \quad (39)$$

Consequently the Green tensor assumes the logarithmic form characteristic of two-dimensional hydrodynamics,

$$G_{ij}(\mathbf{r}) \simeq \frac{1}{8\pi(4\eta_s^2 + \eta_o^2)} \left[\eta_s \left(-3 - 10\gamma + 10 \ln \frac{2}{mr} \right) \delta_{ij} + 6\eta_s \hat{r}_i \hat{r}_j + 4\eta_o \left(\gamma - \ln \frac{2}{mr} \right) \varepsilon_{ij} \right]. \quad (40)$$

Substituting this result into the general dipole velocity formula (9) yields the leading near-field dipolar flow,

$$\mathbf{v}(\mathbf{r}) = \frac{\sigma}{8\pi(4\eta_s^2 + \eta_o^2)} \frac{1}{r} \left[-4\eta_s \alpha \mathbf{d} + 6\eta_s(1 - 2\alpha^2)\hat{\mathbf{r}} + 4\eta_o \alpha \mathbf{d}_\perp \right], \quad (41)$$

where $\mathbf{d}_\perp = \varepsilon \mathbf{d}$. The first two terms correspond to the usual even-viscous dipolar flow, while the third term represents a transverse contribution generated entirely by the odd viscosity.

Using the vorticity expression (10), the corresponding near-field vorticity becomes

$$\omega(\mathbf{r}) = \frac{\sigma}{2\pi(4\eta_s^2 + \eta_o^2)} \frac{\eta_o(\alpha^2 - \beta^2) + 8\eta_s \alpha \beta}{r^2}. \quad (42)$$

Expressed in polar coordinates, where $\alpha = \cos(\theta - \phi)$ and $\beta = \sin(\theta - \phi)$, the vorticity takes the compact angular form

$$\omega(r, \theta, \phi) = \frac{\sigma}{2\pi(4\eta_s^2 + \eta_o^2)} \frac{\eta_o \cos 2(\theta - \phi) + 4\eta_s \sin 2(\theta - \phi)}{r^2}. \quad (43)$$

Thus the degenerate near field retains the logarithmic structure of two-dimensional hydrodynamics. The dipolar velocity decays as r^{-1} while the vorticity exhibits a quadrupolar r^{-2} structure. Odd viscosity generates a transverse component of the dipolar flow and rotates the vorticity quadrupole, producing a characteristic chiral distortion of the flow pattern.

2. Far field

We now turn to the opposite asymptotic regime in which the observation point lies far from the dipole,

$$mr \gg 1.$$

In this limit the modified Bessel functions exhibit the large-argument behavior

$$K_\nu(z) \simeq \sqrt{\frac{\pi}{2z}} e^{-z} \left(1 + \frac{4\nu^2 - 1}{8z} + \mathcal{O}(z^{-2}) \right).$$

Substituting these expansions into the degenerate coefficients $A_0(r)$, $A_1(r)$, and $A_2(r)$ yields

$$A_0(r) = -\frac{3\eta_s}{2\pi(4\eta_s^2 + \eta_o^2)} \frac{1}{m^2 r^2} + \frac{\sqrt{2\pi} \eta_s (9 + 4mr(5 + 8mr))}{32\pi(4\eta_s^2 + \eta_o^2)(mr)^{5/2}} e^{-mr}, \quad (44)$$

$$A_1(r) = \frac{3\eta_s}{\pi(4\eta_s^2 + \eta_o^2)} \frac{1}{m^2 r^2} - \frac{3\sqrt{2\pi} \eta_s (6 + mr(15 + 8mr))}{32\pi(4\eta_s^2 + \eta_o^2)(mr)^{5/2}} e^{-mr}, \quad (45)$$

$$A_2(r) = \frac{\eta_o}{16\sqrt{2\pi}(4\eta_s^2 + \eta_o^2)} \frac{(1 - 8mr)e^{-mr}}{(mr)^{3/2}}. \quad (46)$$

Thus the even sector of the Green tensor retains a long-range algebraic tail proportional to r^{-2} , while the odd sector is exponentially screened by the common screening length $\ell = 1/m$.

Substituting these asymptotic forms into the general velocity expression (9) gives the leading far-field dipolar velocity,

$$\mathbf{v}(\mathbf{r}) \simeq \frac{3\sigma\eta_s}{\pi(4\eta_s^2 + \eta_o^2)} \frac{1}{m^2 r^3} [2\alpha \mathbf{d} + (1 - 4\alpha^2)\hat{\mathbf{r}}] + \mathcal{O}(e^{-mr}). \quad (47)$$

The velocity therefore decays algebraically as r^{-3} , reflecting the long-range dipolar structure of the even-viscosity component of the Green tensor.

The vorticity may be obtained from the invariant expression (10). Substituting the algebraic parts of A_0 and A_1 shows that the leading r^{-2} contributions cancel identically in the vorticity operator,

$$A_0'' - \frac{A_0'}{r} - \frac{A_1'}{r} + \frac{2A_1}{r^2} = 0.$$

Consequently the algebraic contributions cancel in the vorticity operator,

$$A_0'' - \frac{A_0'}{r} - \frac{A_1'}{r} + \frac{2A_1}{r^2} = 0,$$

so that the far-field vorticity is determined entirely by the exponentially small screened terms originating from the Bessel functions. Expanding the resulting expression for large r yields

$$\omega(\mathbf{r}) \simeq \frac{2\sigma\eta_s}{\sqrt{2\pi}(4\eta_s^2 + \eta_o^2)} \alpha\beta m^{3/2} \frac{e^{-mr}}{\sqrt{r}}. \quad (48)$$

IV. DYNAMICAL SYSTEM FOR INTERACTING FORCE DIPOLES ON THE MEMBRANE

The velocity and vorticity fields generated by a single force dipole derived above allow us to formulate the dynamics of a system of interacting dipoles embedded in the membrane.

Consider a collection of N force dipoles labeled by $a = 1, \dots, N$. Each dipole is characterized by its position $R_{ai}(t)$, orientation $d_{ai}(t)$, and dipole strength σ_a . The orientation vector is normalized,

$$d_{ai}d_{ai} = 1. \quad (49)$$

For two dipoles a and b we define the relative separation

$$r_{ab,i} = R_{ai} - R_{bi}, \quad r_{ab} = |\mathbf{r}_{ab}| = \sqrt{r_{ab,i}r_{ab,i}}, \quad \hat{r}_{ab,i} = \frac{r_{ab,i}}{r_{ab}}. \quad (50)$$

The rotational invariants that characterize the relative orientation of dipole b with respect to the separation direction are

$$\alpha_{ab} = d_{bi}\hat{r}_{ab,i}, \quad \beta_{ab} = \varepsilon_{ij}d_{bj}\hat{r}_{ab,i}, \quad (51)$$

which satisfy $\alpha_{ab}^2 + \beta_{ab}^2 = 1$. Using the single-dipole solution derived above, the velocity induced by dipole b at the position of dipole a is

$$v_{ab,i} = \sigma_b \left[\alpha_{ab} \left(A'_0(r_{ab}) + \frac{A_1(r_{ab})}{r_{ab}} \right) d_{bi} \right. \quad (52)$$

$$\left. + \left(\frac{A_1(r_{ab})}{r_{ab}} + \alpha_{ab}^2 \left(A'_1(r_{ab}) - \frac{2A_1(r_{ab})}{r_{ab}} \right) \right) \hat{r}_{ab,i} \right. \quad (53)$$

$$\left. + \alpha_{ab} A'_2(r_{ab}) \varepsilon_{ij} d_{bj} \right]. \quad (54)$$

Each dipole is advected by the velocity generated by all other dipoles,

$$\dot{R}_{ai} = \sum_{b \neq a} v_{ab,i}. \quad (55)$$

The vorticity produced by dipole b at the position of dipole a follows from the single-dipole expression,

$$\omega_{ab} = \sigma_b \left[\alpha_{ab} \beta_{ab} \left(A''_0(r_{ab}) - \frac{A'_0(r_{ab})}{r_{ab}} - \frac{A'_1(r_{ab})}{r_{ab}} + \frac{2A_1(r_{ab})}{r_{ab}^2} \right) \right. \quad (56)$$

$$\left. - \left(\frac{A'_2(r_{ab})}{r_{ab}} \beta_{ab}^2 + \alpha_{ab}^2 A''_2(r_{ab}) \right) \right]. \quad (57)$$

The total vorticity acting on dipole a is therefore

$$\omega_a = \sum_{b \neq a} \omega_{ab}. \quad (58)$$

The orientation of each dipole rotates with the local vorticity of the flow. The angular velocity of a material vector equals one half of the fluid vorticity, leading to

$$\dot{d}_{ai} = \frac{1}{2} \omega_a \varepsilon_{ij} d_{aj}, \quad (59)$$

which preserves the normalization $d_{ai}d_{ai} = 1$.

The interacting force-dipole dynamics on the membrane is therefore described by the coupled system

$$\dot{R}_{ai} = \sum_{b \neq a} v_{ab,i}, \quad (60)$$

$$\dot{d}_{ai} = \frac{1}{2} \omega_a \varepsilon_{ij} d_{aj}, \quad (61)$$

where the pairwise velocity $v_{ab,i}$ and vorticity ω_{ab} are determined entirely by the Green tensor functions $A_0(r)$, $A_1(r)$ and $A_2(r)$. The dynamical system described above possesses only a limited set of exact invariants. The orientation equation

$$\dot{d}_{ai} = \frac{1}{2} \omega_a \varepsilon_{ij} d_{aj}$$

preserves the normalization of each dipole orientation vector, since

$$\frac{d}{dt}(d_{ai}d_{ai}) = 2d_{ai}\dot{d}_{ai} = \omega_a d_{ai}\varepsilon_{ij}d_{aj} = 0,$$

and therefore $d_{ai}d_{ai} = 1$ for all time. Apart from this trivial constraint, the interacting N -dipole system does not generally admit additional conserved quantities. Although the equations of motion are invariant under global translations and rotations of the membrane, these symmetries do not produce conserved linear or angular momenta because the dynamics is driven by active stresses rather than inertial forces. In particular, the center of mass $R_{\text{cm},i} = \frac{1}{N} \sum_a R_{ai}$ evolves according to

$$\dot{R}_{\text{cm},i} = \frac{1}{N} \sum_a \sum_{b \neq a} v_{ab,i},$$

which does not vanish in general since the pairwise velocities $v_{ab,i}$ and $v_{ba,i}$ are not antisymmetric for active dipoles. Consequently the system lacks a conserved energy or momentum and the many-body dynamics is generically dissipative. Additional invariants may nevertheless arise in special situations, such as for two identical dipoles or in particular limits of the Green tensor where the interaction kernel acquires additional symmetries. In particular, in the far-field regime of the incompressible limit, where the leading vorticity contribution vanishes, the dynamics reduces to a purely positional interaction and admits an exact Hamiltonian description, as recently demonstrated in [37], see also [49]. Moreover, for systems with quenched dipole orientations in the incompressible limit, the dynamics can admit a Hamiltonian formulation even in the near field, since the evolution then reduces to a closed system for the dipole positions alone [37].

A. COM drift and Polarization evolution equations

We may also derive evolution equations for global observables of the dipole ensemble. The center of mass of the system is defined by

$$R_{\text{cm},i} = \frac{1}{N} \sum_{a=1}^N R_{ai}.$$

Using the positional dynamics $\dot{R}_{ai} = \sum_{b \neq a} v_{ab,i}$ we obtain

$$\dot{R}_{\text{cm},i} = \frac{1}{N} \sum_a \sum_{b \neq a} v_{ab,i}.$$

Substituting the pair velocity expression gives

$$\begin{aligned} \dot{R}_{\text{cm},i} = \frac{1}{N} \sum_a \sum_{b \neq a} \sigma_b \left[\alpha_{ab} \left(A'_0(r_{ab}) + \frac{A_1(r_{ab})}{r_{ab}} \right) d_{bi} + \left(\frac{A_1(r_{ab})}{r_{ab}} + \alpha_{ab}^2 \left(A'_1(r_{ab}) - \frac{2A_1(r_{ab})}{r_{ab}} \right) \right) \hat{r}_{ab,i} \right. \\ \left. + \alpha_{ab} A'_2(r_{ab}) \varepsilon_{ij} d_{bj} \right]. \end{aligned} \quad (62)$$

Thus the center of mass motion is generated by the collective hydrodynamic interactions among the dipoles and does not generally vanish for active stresses.

The total polarization of the system is defined by

$$P_i = \sum_{a=1}^N d_{ai}.$$

Using the orientation equation $\dot{d}_{ai} = \frac{1}{2} \omega_a \varepsilon_{ij} d_{aj}$ we obtain

$$\dot{P}_i = \frac{1}{2} \sum_a \omega_a \varepsilon_{ij} d_{aj} = \frac{1}{2} \sum_a \sum_{b \neq a} \omega_{ab} \varepsilon_{ij} d_{aj}.$$

Substituting the pair vorticity expression yields

$$\dot{P}_i = \frac{1}{2} \sum_a \sum_{b \neq a} \sigma_b \left[\alpha_{ab} \beta_{ab} \left(A''_0 - \frac{A'_0}{r_{ab}} - \frac{A'_1}{r_{ab}} + \frac{2A_1}{r_{ab}^2} \right) - \left(\frac{A'_2}{r_{ab}} \beta_{ab}^2 + \alpha_{ab}^2 A''_2 \right) \right] \varepsilon_{ij} d_{aj}.$$

These equations show that the center of mass evolves through the collective hydrodynamic velocities while the total polarization rotates under the vorticity field generated by the dipoles.

B. Pair Geometry

It is convenient to describe the relative configuration of two dipoles in terms of the pair separation r_{ab} and the orientation scalars

$$\alpha_{ab} = d_{bi}\hat{r}_{ab,i}, \quad \beta_{ab} = \varepsilon_{ij}d_{bj}\hat{r}_{ab,i},$$

which satisfy $\alpha_{ab}^2 + \beta_{ab}^2 = 1$.

The relative velocity between the dipoles is

$$\Delta V_{ab,i} := \dot{R}_{ai} - \dot{R}_{bi} = v_{ab,i} - v_{ba,i} + \sum_{c \neq a,b} (v_{ac,i} - v_{bc,i}),$$

where the first two terms represent the direct interaction between the pair and the remaining sum accounts for advection by the other dipoles.

The pair geometry evolves according to

$$\begin{aligned} \dot{r}_{ab} &= \hat{r}_{ab,i} \Delta V_{ab,i}, \\ \dot{\alpha}_{ab} &= \frac{1}{2} \omega_b \beta_{ab} + \frac{1}{r_{ab}} (d_{bi} - \alpha_{ab} \hat{r}_{ab,i}) \Delta V_{ab,i}, \\ \dot{\beta}_{ab} &= -\frac{1}{2} \omega_b \alpha_{ab} + \frac{1}{r_{ab}} (\varepsilon_{ij} d_{bj} - \beta_{ab} \hat{r}_{ab,i}) \Delta V_{ab,i}. \end{aligned}$$

Using the explicit dipole velocity field, the radial evolution becomes

$$\begin{aligned} \dot{r}_{ab} &= \sigma_b \left[\alpha_{ab}^2 (A'_0(r_{ab}) + A'_1(r_{ab})) + \beta_{ab}^2 \frac{A_1(r_{ab})}{r_{ab}} + \alpha_{ab} \beta_{ab} A'_2(r_{ab}) \right] \\ &+ \sigma_a \left[\alpha_{ba}^2 (A'_0(r_{ab}) + A'_1(r_{ab})) + \beta_{ba}^2 \frac{A_1(r_{ab})}{r_{ab}} + \alpha_{ba} \beta_{ba} A'_2(r_{ab}) \right] \\ &+ \hat{r}_{ab,i} \sum_{c \neq a,b} (v_{ac,i} - v_{bc,i}). \end{aligned}$$

The orientation scalars evolve according to

$$\begin{aligned} \dot{\alpha}_{ab} &= \frac{1}{2} \omega_b \beta_{ab} + \frac{\sigma_b \alpha_{ab}}{r_{ab}} \left[\beta_{ab}^2 \left(A'_0(r_{ab}) + \frac{A_1(r_{ab})}{r_{ab}} \right) - \alpha_{ab} \beta_{ab} A'_2(r_{ab}) \right] \\ &- \frac{1}{r_{ab}} (d_{bi} - \alpha_{ab} \hat{r}_{ab,i}) v_{ba,i} + \frac{1}{r_{ab}} (d_{bi} - \alpha_{ab} \hat{r}_{ab,i}) \sum_{c \neq a,b} (v_{ac,i} - v_{bc,i}), \\ \dot{\beta}_{ab} &= -\frac{1}{2} \omega_b \alpha_{ab} + \frac{\sigma_b}{r_{ab}} \left[-\alpha_{ab}^2 \beta_{ab} \left(A'_0(r_{ab}) + \frac{A_1(r_{ab})}{r_{ab}} \right) + \alpha_{ab}^3 A'_2(r_{ab}) \right] \\ &- \frac{1}{r_{ab}} (\varepsilon_{ij} d_{bj} - \beta_{ab} \hat{r}_{ab,i}) v_{ba,i} + \frac{1}{r_{ab}} (\varepsilon_{ij} d_{bj} - \beta_{ab} \hat{r}_{ab,i}) \sum_{c \neq a,b} (v_{ac,i} - v_{bc,i}). \end{aligned}$$

These equations show that the pair geometry evolves through three distinct mechanisms: direct dipole–dipole interactions, advection by the background flow generated by the remaining dipoles, and rotation of the dipole orientations by the local vorticity field.

V. SPECIALIZATION TO THE TWO-DIPOLE SYSTEM

We now specialize the general N -dipole dynamics to the case of two interacting dipoles, labeled by $a = 1, 2$. Their positions and orientations are denoted by R_{1i}, R_{2i} and d_{1i}, d_{2i} , with fixed dipole strengths σ_1, σ_2 . It is convenient to introduce the relative separation vector

$$r_i := R_{1i} - R_{2i}, \quad r = |\mathbf{r}|, \quad \hat{r}_i = \frac{r_i}{r}.$$

The geometry of the pair is characterized by the scalars

$$\alpha_{12} = d_{2i}\hat{r}_i, \quad \beta_{12} = \varepsilon_{ij}d_{2j}\hat{r}_i,$$

and

$$\alpha_{21} = d_{1i}\hat{r}_{21,i} = -d_{1i}\hat{r}_i, \quad \beta_{21} = \varepsilon_{ij}d_{1j}\hat{r}_{21,i} = -\varepsilon_{ij}d_{1j}\hat{r}_i.$$

These satisfy

$$\alpha_{12}^2 + \beta_{12}^2 = 1, \quad \alpha_{21}^2 + \beta_{21}^2 = 1.$$

Since there are only two dipoles, the translational equations reduce to

$$\dot{R}_{1i} = v_{12,i}, \quad \dot{R}_{2i} = v_{21,i},$$

where

$$v_{12,i} = \sigma_2 \left[\alpha_{12} \left(A_0'(r) + \frac{A_1(r)}{r} \right) d_{2i} + \left(\frac{A_1(r)}{r} + \alpha_{12}^2 \left(A_1'(r) - \frac{2A_1(r)}{r} \right) \right) \hat{r}_i + \alpha_{12} A_2'(r) \varepsilon_{ij} d_{2j} \right],$$

and

$$v_{21,i} = \sigma_1 \left[\alpha_{21} \left(A_0'(r) + \frac{A_1(r)}{r} \right) d_{1i} - \left(\frac{A_1(r)}{r} + \alpha_{21}^2 \left(A_1'(r) - \frac{2A_1(r)}{r} \right) \right) \hat{r}_i + \alpha_{21} A_2'(r) \varepsilon_{ij} d_{1j} \right].$$

The minus sign in the second line follows from $\hat{r}_{21,i} = -\hat{r}_i$.

The vorticities acting on the two dipoles are simply

$$\omega_1 = \omega_{12}, \quad \omega_2 = \omega_{21},$$

with

$$\omega_{12} = \sigma_2 \left[\alpha_{12} \beta_{12} \left(A_0''(r) - \frac{A_0'(r)}{r} - \frac{A_1'(r)}{r} + \frac{2A_1(r)}{r^2} \right) - \left(\frac{A_2'(r)}{r} \beta_{12}^2 + \alpha_{12}^2 A_2''(r) \right) \right],$$

and

$$\omega_{21} = \sigma_1 \left[\alpha_{21} \beta_{21} \left(A_0''(r) - \frac{A_0'(r)}{r} - \frac{A_1'(r)}{r} + \frac{2A_1(r)}{r^2} \right) - \left(\frac{A_2'(r)}{r} \beta_{21}^2 + \alpha_{21}^2 A_2''(r) \right) \right].$$

The orientation dynamics therefore becomes

$$\dot{d}_{1i} = \frac{1}{2} \omega_{12} \varepsilon_{ij} d_{1j}, \quad \dot{d}_{2i} = \frac{1}{2} \omega_{21} \varepsilon_{ij} d_{2j}.$$

It is often preferable to work directly with the relative coordinate r_i and the center of mass

$$R_{\text{cm},i} = \frac{1}{2} (R_{1i} + R_{2i}).$$

Their evolution is

$$\dot{r}_i = \dot{R}_{1i} - \dot{R}_{2i} = v_{12,i} - v_{21,i}, \quad \dot{R}_{\text{cm},i} = \frac{1}{2} (v_{12,i} + v_{21,i}).$$

Substituting the explicit velocities yields

$$\begin{aligned} \dot{r}_i = & \sigma_2 \left[\alpha_{12} \left(A_0'(r) + \frac{A_1(r)}{r} \right) d_{2i} + \left(\frac{A_1(r)}{r} + \alpha_{12}^2 \left(A_1'(r) - \frac{2A_1(r)}{r} \right) \right) \hat{r}_i + \alpha_{12} A_2'(r) \varepsilon_{ij} d_{2j} \right] \\ & - \sigma_1 \left[\alpha_{21} \left(A_0'(r) + \frac{A_1(r)}{r} \right) d_{1i} - \left(\frac{A_1(r)}{r} + \alpha_{21}^2 \left(A_1'(r) - \frac{2A_1(r)}{r} \right) \right) \hat{r}_i + \alpha_{21} A_2'(r) \varepsilon_{ij} d_{1j} \right], \end{aligned}$$

and

$$\begin{aligned} \dot{R}_{\text{cm},i} = & \frac{1}{2} \sigma_2 \left[\alpha_{12} \left(A_0'(r) + \frac{A_1(r)}{r} \right) d_{2i} + \left(\frac{A_1(r)}{r} + \alpha_{12}^2 \left(A_1'(r) - \frac{2A_1(r)}{r} \right) \right) \hat{r}_i + \alpha_{12} A_2'(r) \varepsilon_{ij} d_{2j} \right] \\ & + \frac{1}{2} \sigma_1 \left[\alpha_{21} \left(A_0'(r) + \frac{A_1(r)}{r} \right) d_{1i} - \left(\frac{A_1(r)}{r} + \alpha_{21}^2 \left(A_1'(r) - \frac{2A_1(r)}{r} \right) \right) \hat{r}_i + \alpha_{21} A_2'(r) \varepsilon_{ij} d_{1j} \right]. \end{aligned}$$

Because there are no additional dipoles, the pair-geometry subsystem closes exactly.

Defining

$$\Delta V_i := \dot{r}_i = v_{12,i} - v_{21,i},$$

we obtain

$$\begin{aligned}\dot{r} &= \hat{r}_i \Delta V_i, \\ \dot{\alpha}_{12} &= \frac{1}{2} \omega_{21} \beta_{12} + \frac{1}{r} (d_{2i} - \alpha_{12} \hat{r}_i) \Delta V_i, \\ \dot{\beta}_{12} &= -\frac{1}{2} \omega_{21} \alpha_{12} + \frac{1}{r} (\varepsilon_{ij} d_{2j} - \beta_{12} \hat{r}_i) \Delta V_i.\end{aligned}$$

Similarly,

$$\begin{aligned}\dot{\alpha}_{21} &= \frac{1}{2} \omega_{12} \beta_{21} - \frac{1}{r} (d_{1i} + \alpha_{21} \hat{r}_i) \Delta V_i, \\ \dot{\beta}_{21} &= -\frac{1}{2} \omega_{12} \alpha_{21} - \frac{1}{r} (\varepsilon_{ij} d_{1j} + \beta_{21} \hat{r}_i) \Delta V_i.\end{aligned}$$

The radial evolution simplifies to

$$\begin{aligned}\dot{r} &= \sigma_2 \left[\alpha_{12}^2 (A'_0(r) + A'_1(r)) + \beta_{12}^2 \frac{A_1(r)}{r} + \alpha_{12} \beta_{12} A'_2(r) \right] \\ &+ \sigma_1 \left[\alpha_{21}^2 (A'_0(r) + A'_1(r)) + \beta_{21}^2 \frac{A_1(r)}{r} + \alpha_{21} \beta_{21} A'_2(r) \right].\end{aligned}$$

The alignment scalars satisfy

$$\begin{aligned}\dot{\alpha}_{12} &= \frac{1}{2} \omega_{21} \beta_{12} + \frac{\sigma_2 \alpha_{12}}{r} \left[\beta_{12}^2 \left(A'_0(r) + \frac{A_1(r)}{r} \right) - \alpha_{12} \beta_{12} A'_2(r) \right] \\ &- \frac{1}{r} (d_{2i} - \alpha_{12} \hat{r}_i) v_{21,i},\end{aligned}$$

and

$$\begin{aligned}\dot{\beta}_{12} &= -\frac{1}{2} \omega_{21} \alpha_{12} + \frac{\sigma_2}{r} \left[-\alpha_{12}^2 \beta_{12} \left(A'_0(r) + \frac{A_1(r)}{r} \right) + \alpha_{12}^3 A'_2(r) \right] \\ &- \frac{1}{r} (\varepsilon_{ij} d_{2j} - \beta_{12} \hat{r}_i) v_{21,i}.\end{aligned}$$

The corresponding equations for $(\alpha_{21}, \beta_{21})$ follow by interchanging $1 \leftrightarrow 2$.

Thus, in the two-dipole case, the many-body problem reduces to a closed nonlinear system for the center of mass, relative separation, and the two dipole orientations. In particular, the relative dynamics is fully determined by the scalar Green-tensor kernels $A_0(r)$, $A_1(r)$, and $A_2(r)$. Finally the polarization evolution becomes

$$\dot{P}_i = \frac{1}{2} \left[\sigma_2 \left(\alpha_{12} \beta_{12} Q(r) - \frac{A'_2(r)}{r} \beta_{12}^2 - \alpha_{12}^2 A''_2(r) \right) \varepsilon_{ij} d_{1j} + \sigma_1 \left(\alpha_{21} \beta_{21} Q(r) - \frac{A'_2(r)}{r} \beta_{21}^2 - \alpha_{21}^2 A''_2(r) \right) \varepsilon_{ij} d_{2j} \right], \quad (63)$$

where

$$Q(r) = A''_0(r) - \frac{A'_0(r)}{r} - \frac{A'_1(r)}{r} + \frac{2A_1(r)}{r^2}.$$

Equivalently, in terms of the pair vorticities ω_{12} and ω_{21} ,

$$\dot{P}_i = \frac{1}{2} (\omega_{12} \varepsilon_{ij} d_{1j} + \omega_{21} \varepsilon_{ij} d_{2j}). \quad (64)$$

VI. TWO-DIPOLE DYNAMICS IN THE NEAR-FIELD DEGENERATE LIMIT

We now specialize the interacting dipole dynamics to the near-field regime of the degenerate Green tensor. In this limit the screening lengths coincide and the real-space Green tensor reduces to a logarithmic form. The leading behavior of the radial kernels for $r \ll m^{-1}$ is

$$A_0(r) \simeq -\frac{5\eta_s}{4\pi(4\eta_s^2 + \eta_o^2)} \ln(mr), \quad (65)$$

$$A_1(r) \simeq \frac{3\eta_s}{4\pi(4\eta_s^2 + \eta_o^2)}, \quad (66)$$

$$A_2(r) \simeq \frac{\eta_o}{2\pi(4\eta_s^2 + \eta_o^2)} \ln(mr). \quad (67)$$

For later convenience we define the denominator

$$D = 4\eta_s^2 + \eta_o^2.$$

The derivatives entering the velocity and vorticity fields therefore reduce to

$$\begin{aligned} A'_0(r) &= -\frac{5\eta_s}{4\pi D} \frac{1}{r}, & A'_1(r) &= 0, & A'_2(r) &= \frac{\eta_o}{2\pi D} \frac{1}{r}, \\ A''_2(r) &= -\frac{\eta_o}{2\pi D} \frac{1}{r^2}, & Q(r) &= A''_0 - \frac{A'_0}{r} - \frac{A'_1}{r} + \frac{2A_1}{r^2} = \frac{4\eta_s}{\pi D} \frac{1}{r^2}. \end{aligned} \quad (68)$$

Considering two dipoles with positions R_1, R_2 , orientations d_1, d_2 , and strengths σ_1, σ_2 . We define the separation vector

$$\mathbf{r} = R_1 - R_2, \quad r = |\mathbf{r}|, \quad \hat{\mathbf{r}} = \mathbf{r}/r.$$

The pair geometry is characterized by the scalars

$$\begin{aligned} \alpha_{12} &= d_2 \cdot \hat{\mathbf{r}}, & \beta_{12} &= (\varepsilon \cdot d_2) \cdot \hat{\mathbf{r}}, \\ \alpha_{21} &= -d_1 \cdot \hat{\mathbf{r}}, & \beta_{21} &= -(\varepsilon \cdot d_1) \cdot \hat{\mathbf{r}}, \end{aligned}$$

together with the dipole-dipole alignment scalars

$$\gamma = d_1 \cdot d_2, \quad \delta = (\varepsilon \cdot d_1) \cdot d_2.$$

In the near-field limit the pair velocities take the form

$$\begin{aligned} v_{12} &= \frac{\sigma_2}{r} \left[-\frac{\eta_s}{2\pi D} \alpha_{12} d_2 + \frac{3\eta_s}{4\pi D} (1 - 2\alpha_{12}^2) \hat{\mathbf{r}} + \frac{\eta_o}{2\pi D} \alpha_{12} (\varepsilon \cdot d_2) \right], \\ v_{21} &= \frac{\sigma_1}{r} \left[-\frac{\eta_s}{2\pi D} \alpha_{21} d_1 - \frac{3\eta_s}{4\pi D} (1 - 2\alpha_{21}^2) \hat{\mathbf{r}} + \frac{\eta_o}{2\pi D} \alpha_{21} (\varepsilon \cdot d_1) \right]. \end{aligned}$$

The relative separation evolves according to

$$\dot{r} = \hat{\mathbf{r}} \cdot (v_{12} - v_{21}),$$

which yields

$$\dot{r} = \frac{1}{4\pi D r} \left[-8\eta_s(\sigma_2\alpha_{12}^2 + \sigma_1\alpha_{21}^2) + 2\eta_o(\sigma_2\alpha_{12}\beta_{12} + \sigma_1\alpha_{21}\beta_{21}) + 3\eta_s(\sigma_1 + \sigma_2) \right]. \quad (69)$$

The vorticities generated by the dipoles reduce to

$$\begin{aligned} \omega_{12} &= \frac{\sigma_2}{2\pi D r^2} (\eta_o(\alpha_{12}^2 - \beta_{12}^2) + 8\eta_s\alpha_{12}\beta_{12}), \\ \omega_{21} &= \frac{\sigma_1}{2\pi D r^2} (\eta_o(\alpha_{21}^2 - \beta_{21}^2) + 8\eta_s\alpha_{21}\beta_{21}). \end{aligned} \quad (70)$$

The orientation vectors rotate according to

$$\dot{d}_1 = \frac{1}{2}\omega_{12}(\varepsilon \cdot d_1), \quad \dot{d}_2 = \frac{1}{2}\omega_{21}(\varepsilon \cdot d_2).$$

It is often convenient to express the orientation dynamics in terms of the alignment scalars.

Using

$$\begin{aligned} \dot{\alpha}_{12} &= \frac{1}{2}\omega_{21}\beta_{12} + \frac{1}{r}(d_2 - \alpha_{12}\hat{r}) \cdot (v_{12} - v_{21}), \\ \dot{\beta}_{12} &= -\frac{1}{2}\omega_{21}\alpha_{12} + \frac{1}{r}(\varepsilon \cdot d_2 - \beta_{12}\hat{r}) \cdot (v_{12} - v_{21}), \end{aligned}$$

and evaluating the projections explicitly in the near-field limit, one finds

$$\begin{aligned} (d_2 - \alpha_{12}\hat{r}) \cdot v_{21} &= \frac{\sigma_1\alpha_{21}}{r} \left[-\frac{\eta_s}{2\pi D}(\gamma + \alpha_{12}\alpha_{21}) + \frac{\eta_o}{2\pi D}(-\delta + \alpha_{12}\beta_{21}) \right], \\ (\varepsilon \cdot d_2 - \beta_{12}\hat{r}) \cdot v_{21} &= \frac{\sigma_1\alpha_{21}}{r} \left[-\frac{\eta_s}{2\pi D}(\delta + \beta_{12}\alpha_{21}) + \frac{\eta_o}{2\pi D}(\gamma + \beta_{12}\beta_{21}) \right]. \end{aligned}$$

The structure of these equations reveals two distinct physical contributions. Terms proportional to η_s originate from the symmetric hydrodynamic response of the membrane and depend only on alignment combinations such as γ and $\alpha_{ab}\alpha_{ba}$. In contrast, the odd viscosity η_o enters exclusively through pseudoscalar combinations involving the Levi-Civita tensor, producing chiral couplings proportional to δ and $\alpha_{ab}\beta_{ba}$. These terms break mirror symmetry of the pair dynamics and generate intrinsically chiral relative motion of the dipoles. Substituting these expressions into the pair vorticities yields

$$\begin{aligned} \omega_{12} &= \frac{\sigma_2}{2\pi D r^2} [\eta_o(\alpha_{12}^2 - \beta_{12}^2) + 8\eta_s\alpha_{12}\beta_{12}], \\ \omega_{21} &= \frac{\sigma_1}{2\pi D r^2} [\eta_o(\alpha_{21}^2 - \beta_{21}^2) + 8\eta_s\alpha_{21}\beta_{21}]. \end{aligned}$$

The polarization evolution therefore reduces to

$$\dot{P}_i = \frac{1}{4\pi D r^2} \left[\sigma_2 (\eta_o(\alpha_{12}^2 - \beta_{12}^2) + 8\eta_s \alpha_{12} \beta_{12}) \varepsilon_{ij} d_{1j} + \sigma_1 (\eta_o(\alpha_{21}^2 - \beta_{21}^2) + 8\eta_s \alpha_{21} \beta_{21}) \varepsilon_{ij} d_{2j} \right]. \quad (71)$$

To analyze the structure of the two-dipole dynamics it is convenient to express the system in terms of variables defined relative to the separation vector between the dipoles. Let

$$\mathbf{r} = r \hat{\mathbf{r}}, \quad \hat{\mathbf{r}} = (\cos \theta, \sin \theta),$$

denote the relative separation between dipoles 1 and 2, where $r = |\mathbf{r}|$ and θ is the polar angle of the separation vector. The dipole orientations are described by unit vectors

$$\mathbf{d}_a = (\cos \phi_a, \sin \phi_a), \quad a = 1, 2.$$

It is convenient to introduce orientation angles measured relative to the line of centers,

$$\psi_1 = \phi_1 - \theta, \quad \psi_2 = \phi_2 - \theta.$$

In terms of these variables the geometric scalars that enter the pair interaction simplify to

$$\begin{aligned} \alpha_{12} &= \mathbf{d}_2 \cdot \hat{\mathbf{r}} = \cos \psi_2, & \beta_{12} &= (\boldsymbol{\varepsilon} \cdot \mathbf{d}_2) \cdot \hat{\mathbf{r}} = \sin \psi_2, \\ \alpha_{21} &= -\mathbf{d}_1 \cdot \hat{\mathbf{r}} = -\cos \psi_1, & \beta_{21} &= -(\boldsymbol{\varepsilon} \cdot \mathbf{d}_1) \cdot \hat{\mathbf{r}} = -\sin \psi_1. \end{aligned}$$

Here ε_{ij} denotes the two-dimensional Levi-Civita tensor. The pair dynamics can then be written entirely in terms of the three variables (r, ψ_1, ψ_2) , while the angle θ follows from the relative motion. In the near-field degenerate limit the evolution equations become (obtained using Mathematica)

$$\begin{aligned} \dot{r} &= \frac{-\eta_s(\sigma_1 + \sigma_2) - 4\eta_s(\sigma_1 \cos 2\psi_1 + \sigma_2 \cos 2\psi_2) + \eta_o(\sigma_1 \sin 2\psi_1 + \sigma_2 \sin 2\psi_2)}{4\pi r (\eta_o^2 + 4\eta_s^2)}, \\ \dot{\theta} &= -\frac{\eta_o(\sigma_1 + \sigma_2) + \eta_o(\sigma_1 \cos 2\psi_1 + \sigma_2 \cos 2\psi_2) + \eta_s(\sigma_1 \sin 2\psi_1 + \sigma_2 \sin 2\psi_2)}{4\pi r^2 (\eta_o^2 + 4\eta_s^2)}, \\ \dot{\psi}_1 &= \frac{\eta_o(\sigma_1 + \sigma_2) + \eta_o \sigma_1 \cos 2\psi_1 + 2\eta_o \sigma_2 \cos 2\psi_2 + \eta_s \sigma_1 \sin 2\psi_1 + 5\eta_s \sigma_2 \sin 2\psi_2}{4\pi r^2 (\eta_o^2 + 4\eta_s^2)}, \\ \dot{\psi}_2 &= \frac{\eta_o(\sigma_1 + \sigma_2) + 2\eta_o \sigma_1 \cos 2\psi_1 + \eta_o \sigma_2 \cos 2\psi_2 + 5\eta_s \sigma_1 \sin 2\psi_1 + \eta_s \sigma_2 \sin 2\psi_2}{4\pi r^2 (\eta_o^2 + 4\eta_s^2)}. \quad (72) \end{aligned}$$

The two-dipole dynamics therefore reduces to a three-dimensional nonlinear system for (r, ψ_1, ψ_2) , while θ evolves kinematically from the relative velocity. A notable feature of

this system is the separation of time scales: the radial evolution scales as $\dot{r} \sim r^{-1}$, whereas the angular variables evolve as $\dot{\theta}, \dot{\psi}_a \sim r^{-2}$. Consequently the dipole orientations evolve faster than the separation at small distances, which naturally produces chiral spiralling trajectories in the near-field regime. To further expose the symmetry structure of the two-dipole dynamics it is useful to introduce the sum and difference orientation variables

$$\Sigma = \psi_1 + \psi_2, \quad \Delta = \psi_1 - \psi_2.$$

These variables describe, respectively, the mean orientation of the dipole pair relative to the separation vector and the relative orientation of the two dipoles. In terms of (Σ, Δ) the individual angles become

$$\psi_1 = \frac{\Sigma + \Delta}{2}, \quad \psi_2 = \frac{\Sigma - \Delta}{2}.$$

Using the trigonometric identities

$$\begin{aligned} \cos 2\psi_1 &= \cos(\Sigma + \Delta), & \cos 2\psi_2 &= \cos(\Sigma - \Delta), \\ \sin 2\psi_1 &= \sin(\Sigma + \Delta), & \sin 2\psi_2 &= \sin(\Sigma - \Delta), \end{aligned}$$

the near-field degenerate equations can be rewritten entirely in terms of (r, Σ, Δ) . The radial evolution becomes (obtained using Mathematica)

$$\dot{r} = \frac{-\eta_o\sigma_1 \sin(\Delta + \Sigma) + \eta_o\sigma_2 \sin(\Delta - \Sigma) + 4\eta_s\sigma_1 \cos(\Delta + \Sigma) + 4\eta_s\sigma_2 \cos(\Delta - \Sigma) + \eta_s(\sigma_1 + \sigma_2)}{4\pi r(\eta_o^2 + 4\eta_s^2)}. \quad (73)$$

The polar angular velocity of the separation vector is

$$\dot{\theta} = -\frac{\eta_o\sigma_1 \cos(\Delta + \Sigma) + \eta_o\sigma_2 \cos(\Delta - \Sigma) + \eta_s\sigma_1 \sin(\Delta + \Sigma) - \eta_s\sigma_2 \sin(\Delta - \Sigma) + \eta_o(\sigma_1 + \sigma_2)}{4\pi r^2(\eta_o^2 + 4\eta_s^2)}. \quad (74)$$

The evolution of the orientation variables follows from

$$\dot{\Sigma} = \dot{\psi}_1 + \dot{\psi}_2, \quad \dot{\Delta} = \dot{\psi}_1 - \dot{\psi}_2,$$

which yields

$$\dot{\Sigma} = \frac{3\sigma_1(\eta_o \cos(\Delta + \Sigma) + 2\eta_s \sin(\Delta + \Sigma)) + 3\sigma_2(\eta_o \cos(\Delta - \Sigma) - 2\eta_s \sin(\Delta - \Sigma)) + 2\eta_o(\sigma_1 + \sigma_2)}{4\pi r^2(\eta_o^2 + 4\eta_s^2)}, \quad (75)$$

$$\dot{\Delta} = -\frac{\eta_o\sigma_1 \cos(\Delta + \Sigma) - \eta_o\sigma_2 \cos(\Delta - \Sigma) + 4\eta_s\sigma_1 \sin(\Delta + \Sigma) + 4\eta_s\sigma_2 \sin(\Delta - \Sigma)}{4\pi r^2(\eta_o^2 + 4\eta_s^2)}. \quad (76)$$

The pair dynamics therefore reduces to a closed nonlinear system for the three variables (r, Σ, Δ) , while the polar angle θ evolves kinematically from the instantaneous velocity. The system exhibits a clear separation of time scales,

$$\dot{r} \sim r^{-1}, \quad \dot{\Sigma}, \dot{\Delta}, \dot{\theta} \sim r^{-2},$$

so that the orientation variables evolve more rapidly than the radial separation at small distances. A useful way to analyze the geometry of the relative trajectories is to eliminate the time variable and derive an equation for the separation as a function of the polar angle.

Using

$$\frac{dr}{d\theta} = \frac{\dot{r}}{\dot{\theta}},$$

one obtains (using Mathematica)

$$\frac{dr}{d\theta} = r \frac{-\eta_o \sigma_1 \sin(\Delta + \Sigma) + \eta_o \sigma_2 \sin(\Delta - \Sigma) + 4\eta_s \sigma_1 \cos(\Delta + \Sigma) + 4\eta_s \sigma_2 \cos(\Delta - \Sigma) + \eta_s(\sigma_1 + \sigma_2)}{\eta_o \sigma_1 \cos(\Delta + \Sigma) + \eta_o \sigma_2 \cos(\Delta - \Sigma) + \eta_s \sigma_1 \sin(\Delta + \Sigma) - \eta_s \sigma_2 \sin(\Delta - \Sigma) + \eta_o(\sigma_1 + \sigma_2)}. \quad (77)$$

It is convenient to write this relation in logarithmic form,

$$\frac{d \ln r}{d\theta} = \kappa(\Sigma, \Delta), \quad (78)$$

where the spiral function

$$\kappa(\Sigma, \Delta) = \frac{-\eta_o \sigma_1 \sin(\Delta + \Sigma) + \eta_o \sigma_2 \sin(\Delta - \Sigma) + 4\eta_s \sigma_1 \cos(\Delta + \Sigma) + 4\eta_s \sigma_2 \cos(\Delta - \Sigma) + \eta_s(\sigma_1 + \sigma_2)}{\eta_o \sigma_1 \cos(\Delta + \Sigma) + \eta_o \sigma_2 \cos(\Delta - \Sigma) + \eta_s \sigma_1 \sin(\Delta + \Sigma) - \eta_s \sigma_2 \sin(\Delta - \Sigma) + \eta_o(\sigma_1 + \sigma_2)}$$

controls the radial evolution of the trajectory.

When κ varies slowly along the trajectory the solution locally approximates a logarithmic spiral,

$$r(\theta) \approx r_0 e^{\kappa \theta}.$$

The sign of κ determines the character of the motion. Negative values of κ correspond to spiralling collision trajectories, where the dipoles approach one another while rotating, whereas positive values correspond to spiralling escape trajectories. The odd viscosity coefficient η_o appears in both the numerator and denominator of κ and therefore controls the handedness of the spiral: reversing the sign of η_o reverses the direction of rotation while leaving the radial dynamics unchanged.

These results show that the near-field degenerate dipole interaction naturally generates chiral spiral trajectories whose orientation is set by the sign of the odd viscosity and whose radial behavior is governed by the instantaneous values of the orientation variables (Σ, Δ) .

a. Equal-strength dipoles and spiral dynamics. Additional analytical insight can be obtained in the symmetric case where the dipole strengths are equal,

$$\sigma_1 = \sigma_2 = \sigma.$$

In this case the dynamical system simplifies considerably. The radial evolution becomes

$$\dot{r} = \frac{\eta_o \sigma \cos \Delta \sin \Sigma - 4\eta_s \sigma \cos \Delta \cos \Sigma - \eta_s \sigma}{2\pi r (\eta_o^2 + 4\eta_s^2)}. \quad (79)$$

The angular velocity of the separation vector is

$$\dot{\theta} = -\frac{\sigma [\cos \Delta (\eta_o \cos \Sigma + \eta_s \sin \Sigma) + \eta_o]}{2\pi r^2 (\eta_o^2 + 4\eta_s^2)}. \quad (80)$$

The orientation variables satisfy

$$\dot{\Sigma} = \frac{\sigma [3 \cos \Delta (\eta_o \cos \Sigma + 2\eta_s \sin \Sigma) + 2\eta_o]}{2\pi r^2 (\eta_o^2 + 4\eta_s^2)}, \quad (81)$$

$$\dot{\Delta} = \frac{\sigma \sin \Delta (\eta_o \sin \Sigma - 4\eta_s \cos \Sigma)}{2\pi r^2 (\eta_o^2 + 4\eta_s^2)}. \quad (82)$$

As in the general case, the separation of time scales persists,

$$\dot{r} \sim r^{-1}, \quad \dot{\theta}, \dot{\Sigma}, \dot{\Delta} \sim r^{-2},$$

so that the dipole orientations evolve more rapidly than the radial distance at small separations.

The geometry of the relative trajectories may again be obtained by eliminating the time variable,

$$\frac{dr}{d\theta} = \frac{\dot{r}}{\dot{\theta}}.$$

This yields

$$\frac{dr}{d\theta} = r \frac{-\eta_o \cos \Delta \sin \Sigma + 4\eta_s \cos \Delta \cos \Sigma + \eta_s}{\eta_o \cos \Delta \cos \Sigma + \eta_s \cos \Delta \sin \Sigma + \eta_o}. \quad (83)$$

Equivalently,

$$\frac{d \ln r}{d\theta} = \kappa(\Sigma, \Delta),$$

where the spiral function is

$$\kappa(\Sigma, \Delta) = \frac{-\eta_o \cos \Delta \sin \Sigma + 4\eta_s \cos \Delta \cos \Sigma + \eta_s}{\eta_o \cos \Delta \cos \Sigma + \eta_s \cos \Delta \sin \Sigma + \eta_o}.$$

Although the relation

$$\frac{d \ln r}{d\theta} = \kappa(\Sigma, \Delta)$$

has the form of a spiral equation, the near-field trajectories are not generically logarithmic spirals because Σ and Δ typically evolve by $O(1)$ over the same angular timescale as θ . A logarithmic-spiral approximation is valid only when $\kappa(\Sigma, \Delta)$ is approximately constant along a given trajectory.

$$r(\theta) \approx r_0 e^{\kappa\theta}.$$

The sign of κ determines whether the dipoles spiral toward one another or separate, while the odd viscosity η_o controls the handedness of the spiral through the pseudoscalar combinations appearing in both the numerator and denominator.

VII. TWO-DIPOLE DYNAMICS IN THE FAR-FIELD DEGENERATE LIMIT

We now specialize the general two-dipole dynamical system derived in the previous section to the far-field limit of the degenerate Green tensor. In this regime the dipole separation is large compared with the hydrodynamic screening length,

$$mr \gg 1.$$

The leading algebraic parts of the degenerate Green tensor are

$$A_0(r) = -\frac{C}{r^2}, \quad A_1(r) = \frac{2C}{r^2}, \quad (84)$$

with

$$C = \frac{3\eta_s}{2\pi(4\eta_s^2 + \eta_o^2)m^2}. \quad (85)$$

The antisymmetric component is exponentially screened,

$$A_2(r) = D \frac{(1 - 8mr)e^{-mr}}{(mr)^{3/2}}, \quad D = \frac{\eta_o}{16\sqrt{2\pi}(4\eta_s^2 + \eta_o^2)}. \quad (86)$$

The derivatives entering the dynamical equations are

$$\begin{aligned} A'_0(r) &= \frac{2C}{r^3}, & A'_1(r) &= -\frac{4C}{r^3}, \\ A'_0(r) + \frac{A_1(r)}{r} &= \frac{4C}{r^3}, & A'_1(r) - \frac{2A_1(r)}{r} &= -\frac{8C}{r^3}. \end{aligned}$$

Substituting these expressions into the general dipole velocity law yields the far-field pair velocity

$$v_{ab,i} = \sigma_b \left[\frac{4C}{r^3} \alpha_{ab} d_{bi} + \frac{2C}{r^3} (1 - 4\alpha_{ab}^2) \hat{r}_i + \alpha_{ab} A_2'(r) \varepsilon_{ij} d_{bj} \right].$$

The relative velocity $\dot{r}_i = v_{12,i} - v_{21,i}$ becomes

$$\begin{aligned} \dot{r}_i &= \frac{4C}{r^3} (\sigma_2 \alpha_{12} d_{2i} - \sigma_1 \alpha_{21} d_{1i}) \\ &+ \frac{2C}{r^3} \left[\sigma_2 (1 - 4\alpha_{12}^2) + \sigma_1 (1 - 4\alpha_{21}^2) \right] \hat{r}_i \\ &+ \sigma_2 \alpha_{12} A_2'(r) \varepsilon_{ij} d_{2j} - \sigma_1 \alpha_{21} A_2'(r) \varepsilon_{ij} d_{1j}. \end{aligned} \quad (87)$$

Projecting along the separation direction $\hat{\mathbf{r}}$ gives the radial evolution

$$\dot{r} = \frac{2C}{r^3} \left[(-\alpha_{21}^2 + \beta_{21}^2) \sigma_1 + (-\alpha_{12}^2 + \beta_{12}^2) \sigma_2 \right] + A_2'(r) (\alpha_{21} \beta_{21} \sigma_1 + \alpha_{12} \beta_{12} \sigma_2). \quad (88)$$

It is therefore natural to decompose the radial dynamics into parity-even and parity-odd sectors, $\dot{r} = \dot{r}_{\text{even}} + \dot{r}_{\text{odd}}$. The symmetric contribution reads

$$\dot{r}_{\text{even}} = \frac{2C}{r^3} \left[(-\alpha_{21}^2 + \beta_{21}^2) \sigma_1 + (-\alpha_{12}^2 + \beta_{12}^2) \sigma_2 \right], \quad (89)$$

while the odd-viscosity contribution is

$$\dot{r}_{\text{odd}} = \frac{De^{-mr} m(-3 + 2mr(3 + 8mr))}{2(mr)^{5/2}} (\alpha_{21} \beta_{21} \sigma_1 + \alpha_{12} \beta_{12} \sigma_2). \quad (90)$$

The vorticity acting on each dipole is determined by

$$\omega_{ab} = \sigma_b \left[\alpha_{ab} \beta_{ab} Q(r) - \left(\frac{A_2'(r)}{r} \beta_{ab}^2 + \alpha_{ab}^2 A_2''(r) \right) \right],$$

where

$$Q(r) = A_0'' - \frac{A_0'}{r} - \frac{A_1'}{r} + \frac{2A_1}{r^2}.$$

Using only the leading algebraic far-field pieces

$$A_0(r) = -\frac{C}{r^2}, \quad A_1(r) = \frac{2C}{r^2},$$

the vorticity combination reduces to

$$Q(r) = A_0'' - \frac{A_0'}{r} - \frac{A_1'}{r} + \frac{2A_1}{r^2} = 0. \quad (91)$$

Thus the symmetric sector does not contribute to the dipole rotation at algebraic order in the far field. However, the full far-field expressions for A_0 and A_1 contain exponentially small

corrections proportional to e^{-mr} . Retaining these terms yields a nonvanishing contribution to $Q(r)$. Using the complete expressions for A_0 and A_1 one finds

$$Q(r) = \frac{\eta_s e^{-mr}}{64\sqrt{2\pi}(4\eta_s^2 + \eta_o^2)} \frac{81 + 2mr(-33 + 8mr(6 + mr(15 + 8mr)))}{r^2(mr)^{5/2}}. \quad (92)$$

For large separations $mr \gg 1$ the leading behavior becomes

$$Q(r) \sim \frac{\sqrt{2}}{\sqrt{\pi}} \frac{\eta_s m^{3/2}}{4\eta_s^2 + \eta_o^2} \frac{e^{-mr}}{\sqrt{r}}. \quad (93)$$

This term is exponentially suppressed but nonzero, and it has the same asymptotic scaling as the odd-viscosity contribution arising from $A_2''(r)$,

$$A_2''(r) \sim -8Dm^{3/2} \frac{e^{-mr}}{\sqrt{r}}.$$

Consequently the far-field rotational dynamics receives comparable exponentially small contributions from both the symmetric and antisymmetric sectors of the Green tensor, even though the symmetric contribution vanishes at leading algebraic order. The pair vorticities follow from the general relation

$$\omega_{ab} = \sigma_b \left[\alpha_{ab} \beta_{ab} Q(r) - \left(\frac{A_2'(r)}{r} \beta_{ab}^2 + \alpha_{ab}^2 A_2''(r) \right) \right],$$

where

$$Q(r) = A_0'' - \frac{A_0'}{r} - \frac{A_1'}{r} + \frac{2A_1}{r^2}.$$

Using the full far-field expressions of the degenerate Green tensor, Mathematica yields the explicit result

$$Q(r) = \frac{\eta_s e^{-mr} (81 + 2mr(-33 + 8mr(6 + mr(15 + 8mr))))}{64\sqrt{2\pi} r^2 (mr)^{5/2} (\eta_o^2 + 4\eta_s^2)}. \quad (94)$$

The derivatives of the antisymmetric kernel are

$$A_2'(r) = \frac{De^{-mr} m(-3 + 2mr(3 + 8mr))}{2(mr)^{5/2}}, \quad (95)$$

$$A_2''(r) = \frac{De^{-mr} (15 - 4mr(3 + mr(7 + 8mr)))}{4r^2 (mr)^{3/2}}. \quad (96)$$

Substituting these expressions gives the full pair vorticity

$$\begin{aligned} \omega_{ab} = & \frac{\sigma_b e^{-mr}}{64\sqrt{2\pi} r^2 (mr)^{5/2} (\eta_o^2 + 4\eta_s^2)} \\ & \times \left[\eta_o (mr(-15 + 4mr(3 + mr(7 + 8mr)))) \alpha_{ab}^2 - 2(-3 + 2mr(3 + 8mr)) \beta_{ab}^2 \right. \\ & \left. + \eta_s (81 + 2mr(-33 + 8mr(6 + mr(15 + 8mr)))) \alpha_{ab} \beta_{ab} \right]. \quad (97) \end{aligned}$$

For large separations $mr \gg 1$ the dominant asymptotic behavior becomes

$$\omega_{ab} = \frac{m^{3/2} e^{-mr}}{2\sqrt{2\pi}(\eta_o^2 + 4\eta_s^2)} (\alpha_{ab}^2 \eta_o + 4\alpha_{ab}\beta_{ab}\eta_s) \frac{\sigma_b}{\sqrt{r}} + O\left(\frac{e^{-mr}}{r^{3/2}}\right). \quad (98)$$

It is useful to express the angular dependence in terms of the orientation of dipole b relative to the separation direction. Let

$$\psi_b = \phi_b - \theta$$

denote the angle between the dipole orientation and the line of centers. The geometric scalars entering the pair interaction then reduce to

$$\alpha_{ab} = \cos \psi_b, \quad \beta_{ab} = \sin \psi_b.$$

Substituting these relations into the asymptotic vorticity yields

$$\omega_{ab} = \frac{m^{3/2} e^{-mr} \sigma_b}{2\sqrt{2\pi}(\eta_o^2 + 4\eta_s^2)\sqrt{r}} \left[\frac{\eta_o}{2} (1 + \cos 2\psi_b) + 2\eta_s \sin 2\psi_b \right] + O\left(\frac{e^{-mr}}{r^{3/2}}\right). \quad (99)$$

This representation makes the angular structure of the far-field rotational coupling transparent. The odd viscosity contributes through the even harmonic $(1 + \cos 2\psi_b)$, while the symmetric viscosity generates the chiral component proportional to $\sin 2\psi_b$. Both contributions are exponentially screened with distance, reflecting the short-range character of the rotational interaction in the degenerate far-field regime. The orientation dynamics therefore obeys

$$\dot{d}_{ai} = \frac{1}{2} \omega_a \varepsilon_{ij} d_{aj}, \quad \omega_a = \omega_{ab}.$$

Thus the far-field degenerate two-dipole system exhibits the scalings

$$\begin{aligned} \dot{r}_i &\sim r^{-3}, \\ \dot{r} &\sim r^{-3}, \\ \omega_{ab} &\sim e^{-mr} r^{-1/2}. \end{aligned}$$

The translational interaction therefore decays algebraically as r^{-3} , while the rotational coupling is exponentially suppressed. Although the algebraic symmetric contribution cancels exactly in the far field, the exponentially small corrections to A_0 and A_1 generate a nonvanishing term proportional to η_s in ω_{ab} , so that both the symmetric and antisymmetric sectors contribute at the same asymptotic order. The translational interaction therefore decays algebraically as r^{-3} , while the rotational coupling is exponentially screened and arises entirely from the odd-viscosity sector of the Green tensor.

a. Equal-strength dipoles We now reconsider the far-field dynamics of a pair of identical dipoles in the degenerate regime, retaining the full far-field expressions of the Green tensor rather than truncating to the leading algebraic terms only. We therefore set

$$\sigma_1 = \sigma_2 = \sigma.$$

Let the dipole orientations be described by the laboratory angles ϕ_1 and ϕ_2 , and define the collective variables

$$\Sigma = \phi_1 + \phi_2, \quad \Delta = \phi_1 - \phi_2.$$

The separation direction is

$$\hat{\mathbf{r}} = (\cos \theta, \sin \theta),$$

and we work throughout in the regime

$$mr \gg 1.$$

For convenience, we introduce

$$D = 4\eta_s^2 + \eta_o^2, \quad z = mr,$$

together with the polynomials

$$\begin{aligned} U(z) &= 81 + 2z(-33 + 8z(6 + z(15 + 8z))), \\ P_1(z) &= -3 + 2z(3 + 8z), \\ P_2(z) &= -21 + 4z(6 + z(15 + 8z)), \\ R(z) &= 81 + 8z(21 + z(15 + 8z)), \\ S(z) &= 9 + z(3 - 2z(3 + 8z)), \\ T(z) &= 81 + z(183 + 2z(45 - 8z)). \end{aligned} \tag{100}$$

The full far-field degenerate kernels are (obtained using Mathematica)

$$\begin{aligned} A_0(r) &= -\frac{3\eta_s}{2\pi D} \frac{1}{m^2 r^2} + \frac{\sqrt{2\pi} \eta_s (9 + 4mr(5 + 8mr))}{32\pi D (mr)^{5/2}} e^{-mr}, \\ A_1(r) &= \frac{3\eta_s}{\pi D} \frac{1}{m^2 r^2} - \frac{3\sqrt{2\pi} \eta_s (6 + mr(15 + 8mr))}{32\pi D (mr)^{5/2}} e^{-mr}, \\ A_2(r) &= \frac{\eta_o}{16\sqrt{2\pi} D} \frac{(1 - 8mr)e^{-mr}}{(mr)^{3/2}}. \end{aligned}$$

The combination entering the vorticity formula in the symmetric sector is

$$Q(r) = A_0'' - \frac{A_0'}{r} - \frac{A_1'}{r} + \frac{2A_1}{r^2}.$$

Using the full far-field kernels, one finds

$$Q(r) = \frac{\eta_s e^{-z}}{64\sqrt{2\pi} r^2 z^{5/2} D} U(z).$$

Thus the symmetric sector cancels at algebraic order but reappears through exponentially small corrections. The large-distance expansion is

$$Q(r) \sim \frac{\sqrt{2/\pi} \eta_s m^{3/2} e^{-mr}}{D \sqrt{r}}. \quad (101)$$

The pair vorticities are obtained from

$$\omega_{ab} = \sigma \left[\alpha_{ab} \beta_{ab} Q(r) - \left(\frac{A_2'(r)}{r} \beta_{ab}^2 + \alpha_{ab}^2 A_2''(r) \right) \right].$$

For the full far-field kernels this yields the asymptotic form

$$\omega_{ab} = \frac{m^{3/2} e^{-mr} \sigma}{2\sqrt{2\pi} D} \left(\alpha_{ab}^2 \eta_o + 4\alpha_{ab} \beta_{ab} \eta_s \right) \frac{1}{\sqrt{r}} + O\left(\frac{e^{-mr}}{r^{3/2}}\right). \quad (102)$$

If $\psi_b = \phi_b - \theta$ denotes the orientation of dipole b relative to the line of centers, so that

$$\alpha_{ab} = \cos \psi_b, \quad \beta_{ab} = \sin \psi_b,$$

then the far-field vorticity may equivalently be written as

$$\omega_{ab} = \frac{m^{3/2} e^{-mr} \sigma}{2\sqrt{2\pi} D \sqrt{r}} \left[\frac{\eta_o}{2} (1 + \cos 2\psi_b) + 2\eta_s \sin 2\psi_b \right] + O\left(\frac{e^{-mr}}{r^{3/2}}\right). \quad (103)$$

Hence the rotational coupling is exponentially suppressed, with comparable contributions from the antisymmetric and symmetric sectors at the first nonvanishing order. Substituting the full kernels into the two-dipole velocity law and specializing to equal strengths gives the relative radial and orbital velocities. Writing the result in terms of $(r, \Sigma, \Delta, \theta)$, one finds

$$\begin{aligned} \dot{r} = \frac{\sigma m e^{-z}}{64\pi z^{7/2} D} & \left[-384e^z \sqrt{z} \eta_s \cos \Delta \cos(\Sigma - 2\theta) \right. \\ & + \sqrt{2\pi} \eta_s (S(z) + T(z) \cos \Delta \cos(\Sigma - 2\theta)) \\ & \left. - \sqrt{2\pi} z P_1(z) \eta_o \cos \Delta \sin(\Sigma - 2\theta) \right], \end{aligned} \quad (104)$$

and

$$\dot{\theta} = \frac{\sigma e^{-z}}{64\pi r^2 z^{5/2} D} \left[384e^z \sqrt{z} \eta_s \cos \Delta \sin(\Sigma - 2\theta) + \sqrt{2\pi} \left(z P_1(z) \eta_o (1 + \cos \Delta \cos(\Sigma - 2\theta)) - R(z) \eta_s \cos \Delta \sin(\Sigma - 2\theta) \right) \right]. \quad (105)$$

The orientation dynamics follows from the pair vorticities. In terms of

$$\dot{\Sigma} = \frac{\omega_{12} + \omega_{21}}{2}, \quad \dot{\Delta} = \frac{\omega_{12} - \omega_{21}}{2},$$

the full far-field equal-strength system becomes

$$\dot{\Sigma} = \frac{\sigma e^{-z}}{128\sqrt{2\pi} r^2 z^{5/2} D} \left[z \eta_o (-9 + 4z^2(-1 + 8z) + P_2(z) \cos \Delta \cos(\Sigma - 2\theta)) + U(z) \eta_s \cos \Delta \sin(\Sigma - 2\theta) \right], \quad (106)$$

$$\dot{\Delta} = \frac{\sigma e^{-z} \sin \Delta}{128\sqrt{2\pi} r^2 z^{5/2} D} \left[-U(z) \eta_s \cos(\Sigma - 2\theta) + z P_2(z) \eta_o \sin(\Sigma - 2\theta) \right]. \quad (107)$$

These formulas exhibit the main structural features of the corrected far-field dynamics.

First, the branch

$$\Delta = 0 \quad \text{or} \quad \Delta = \pi$$

remains invariant because $\dot{\Delta}$ carries an overall factor $\sin \Delta$. Second, the translational sector is algebraic, whereas the orientational sector is exponentially weak:

$$\dot{r}_i \sim r^{-3}, \quad \dot{r} \sim r^{-3}, \quad \omega_{ab} \sim e^{-mr} r^{-1/2}, \quad \dot{\Sigma}, \dot{\Delta} \sim e^{-mr} r^{-1/2}.$$

Thus the far-field motion is dominated by algebraic translation, while rotation and orientational relaxation are exponentially slow.

On the invariant branch $\Delta = 0$, the equations reduce to

$$\dot{r}|_{\Delta=0} = \frac{\sigma m e^{-z}}{64\pi z^{7/2} D} \left[(-384e^z \sqrt{z} + \sqrt{2\pi} T(z)) \eta_s \cos(\Sigma - 2\theta) + \sqrt{2\pi} S(z) \eta_s - \sqrt{2\pi} z P_1(z) \eta_o \sin(\Sigma - 2\theta) \right], \quad (108)$$

$$\dot{\theta}|_{\Delta=0} = \frac{\sigma e^{-z}}{64\pi r^2 z^{5/2} D} \left[384e^z \sqrt{z} \eta_s \sin(\Sigma - 2\theta) + \sqrt{2\pi} \left(z P_1(z) \eta_o (1 + \cos(\Sigma - 2\theta)) - R(z) \eta_s \sin(\Sigma - 2\theta) \right) \right], \quad (109)$$

$$\dot{\Sigma}|_{\Delta=0} = \frac{\sigma e^{-z}}{128\sqrt{2\pi} r^2 z^{5/2} D} \left[z \eta_o (-9 + 4z^2(-1 + 8z) + P_2(z) \cos(\Sigma - 2\theta)) + U(z) \eta_s \sin(\Sigma - 2\theta) \right], \quad (110)$$

$$\dot{\Delta}|_{\Delta=0} = 0. \quad (111)$$

Eliminating time between the radial and orbital equations gives the orbital equation $\frac{dr}{d\theta} = \frac{\dot{r}}{\dot{\theta}}$.

On the branch $\Delta = 0$ this becomes

$$\frac{dr}{d\theta} = r \frac{(-384e^z \sqrt{z} + \sqrt{2\pi}T(z))\eta_s \cos \Psi + \sqrt{2\pi}S(z)\eta_s - \sqrt{2\pi}zP_1(z)\eta_o \sin \Psi}{384e^z \sqrt{z}\eta_s \sin \Psi + \sqrt{2\pi}(zP_1(z)\eta_o(1 + \cos \Psi) - R(z)\eta_s \sin \Psi)}, \quad (112)$$

where

$$\Psi = \Sigma - 2\theta.$$

Thus the orbital law has the generic spiral form

$$\frac{dr}{d\theta} = r F(r, \Psi).$$

At leading large distance the algebraic terms dominate and this reduces to

$$\frac{dr}{d\theta} \sim -r \cot \Psi.$$

Hence, when Ψ varies slowly, the orbit is asymptotically logarithmic.

The phase dynamics is obtained from

$$\dot{\Psi} = \dot{\Sigma} - 2\dot{\theta}.$$

Using the above branch equations, one finds that $\dot{\Psi}$ is again exponentially small. Consequently the corrected full far-field picture is the following: algebraic translation persists, while the relative orientation variables evolve only through exponentially suppressed corrections. This slow phase dynamics allows approximate orientation locking and supports asymptotic spiral trajectories, but the locking mechanism is generated by both the symmetric and antisymmetric sectors at the first nonzero order.

Finally, in the convenient gauge $\theta = 0$, the corrected equal-strength system becomes

$$\dot{r} = \frac{\sigma m e^{-z}}{64\pi z^{7/2} D} \left[-384e^z \sqrt{z} \eta_s \cos \Delta \cos \Sigma + \sqrt{2\pi} \eta_s S(z) + \sqrt{2\pi} \cos \Delta (T(z) \eta_s \cos \Sigma - z P_1(z) \eta_o \sin \Sigma) \right], \quad (113)$$

$$\dot{\Sigma} = \frac{\sigma e^{-z}}{128\sqrt{2\pi} r^2 z^{5/2} D} \left[z \eta_o (-9 + 4z^2(-1 + 8z) + P_2(z) \cos \Delta \cos \Sigma) + U(z) \eta_s \cos \Delta \sin \Sigma \right], \quad (114)$$

$$\dot{\Delta} = \frac{\sigma e^{-z} \sin \Delta}{128\sqrt{2\pi} r^2 z^{5/2} D} \left[-U(z) \eta_s \cos \Sigma + z P_2(z) \eta_o \sin \Sigma \right]. \quad (115)$$

These equations provide a compact explicit description of the corrected full far-field equal-strength dynamics in the degenerate regime.

VIII. ODD CONTRIBUTION TO RELATIVE PAIR MOTION AND IDENTIFICATION OF ODD-SECTOR OBSERVABLES

We now examine how the antisymmetric part of the hydrodynamic response influences the dynamics of interacting dipoles. Starting from the general pairwise velocity and vorticity laws derived earlier, we analyze the relative motion of a dipole pair and identify the contributions that arise specifically from the antisymmetric Green-tensor coefficient $A_2(r)$. The analysis is carried out for the full general solution, so that both symmetric and antisymmetric sectors of the response are retained throughout. By separating the terms proportional to $A_2(r)$ and its derivatives, we construct diagnostic quantities that isolate the odd-sector contribution to pair translation, orbital motion, and orientational dynamics. We consider two dipoles labeled 1 and 2 with positions R_{ai} and orientations d_{ai} . Define the relative separation

$$r_i = R_{1i} - R_{2i}, \quad r = |\mathbf{r}|, \quad \hat{r}_i = \frac{r_i}{r}.$$

The relative velocity is

$$\dot{r}_i = v_{12,i} - v_{21,i}.$$

For a dipole pair the geometric scalars

$$\alpha_{ab} = d_{bi} \hat{r}_{ab,i}, \quad \beta_{ab} = \varepsilon_{ij} d_{bj} \hat{r}_{ab,i}$$

describe the orientation of dipole b relative to the separation direction. From the general pairwise velocity law, the part generated by the antisymmetric Green tensor coefficient $A_2(r)$ is

$$v_{ab,i}^{(\text{odd})} = \sigma_b \alpha_{ab} A_2'(r_{ab}) \varepsilon_{ij} d_{bj}.$$

A convenient observable characterizing the relative motion is the transverse velocity

$$V_{\perp} = \varepsilon_{ij} \hat{r}_i \dot{r}_j.$$

Using the pairwise velocity law one finds

$$V_{\perp} = -\left(\sigma_2 \alpha_{12} \beta_{12} + \sigma_1 \alpha_{21} \beta_{21}\right) \left(A_0'(r) + \frac{A_1(r)}{r}\right) - \left(\sigma_2 \alpha_{12}^2 + \sigma_1 \alpha_{21}^2\right) A_2'(r). \quad (116)$$

The first term originates from the symmetric Green tensor coefficients A_0 and A_1 , while the second term arises entirely from the antisymmetric coefficient A_2 . The purely odd

contribution to the transverse pair motion is therefore

$$V_{\perp}^{(\text{odd})} = -\left(\sigma_2\alpha_{12}^2 + \sigma_1\alpha_{21}^2\right)A_2'(r). \quad (117)$$

A related observable is the orbital angular velocity of the pair,

$$\Omega = \frac{1}{r^2}\varepsilon_{ij}r_i\dot{r}_j = \frac{1}{r}V_{\perp}, \quad (118)$$

which gives

$$\Omega = -\frac{1}{r}\left(\sigma_2\alpha_{12}\beta_{12} + \sigma_1\alpha_{21}\beta_{21}\right)\left(A_0'(r) + \frac{A_1(r)}{r}\right) - \frac{1}{r}\left(\sigma_2\alpha_{12}^2 + \sigma_1\alpha_{21}^2\right)A_2'(r). \quad (119)$$

The odd contribution to the orbital rotation is therefore

$$\Omega^{(\text{odd})} = -\frac{1}{r}\left(\sigma_2\alpha_{12}^2 + \sigma_1\alpha_{21}^2\right)A_2'(r). \quad (120)$$

Odd viscosity also influences the orientational dynamics through the vorticity field generated by the dipoles. The orientation of dipole a evolves according to

$$\dot{d}_{ai} = \frac{1}{2}\omega_a\varepsilon_{ij}d_{aj}, \quad \omega_a = \sum_{b \neq a}\omega_{ab}.$$

The antisymmetric contribution to the pairwise vorticity is

$$\omega_{ab}^{(\text{odd})} = -\sigma_b\left[\frac{A_2'(r_{ab})}{r_{ab}}\beta_{ab}^2 + \alpha_{ab}^2A_2''(r_{ab})\right]. \quad (121)$$

A convenient scalar built out of the odd sector is obtained from the difference of the two orientation rates,

$$\Delta\dot{\phi}^{(\text{odd})} = \frac{1}{2}\left(\omega_{12}^{(\text{odd})} - \omega_{21}^{(\text{odd})}\right), \quad (122)$$

which depends only on the radial kernels $A_2'(r)$ and $A_2''(r)$. The full observables V_{\perp} , Ω , and $\dot{\phi}_a$ generally contain both symmetric and antisymmetric contributions. The quantities $V_{\perp}^{(\text{odd})}$, $\Omega^{(\text{odd})}$, and $\omega_{ab}^{(\text{odd})}$ isolate the part of the dynamics generated by the antisymmetric Green-tensor coefficient $A_2(r)$, but they represent extracted components of the full observables rather than standalone single-run measurements.

In practice the antisymmetric contribution may nevertheless be identified experimentally in several ways. First, since the odd viscosity coefficient η_o changes sign under reversal of the medium chirality, comparison of the pair dynamics in systems with opposite chirality isolates the part of the motion proportional to $A_2(r)$ to leading order. Second, in the degenerate model the symmetric and antisymmetric responses exhibit distinct radial dependences:

the symmetric contributions arise from the algebraic kernels $A_0(r)$ and $A_1(r)$, whereas the antisymmetric contribution is controlled by the screened kernel $A_2(r)$ and its derivatives. Measurements of the distance dependence of the pair motion can therefore help separate the two responses. Finally, the theoretical pair dynamics derived above may be fitted to experimentally measured dipole trajectories, allowing the antisymmetric kernel $A_2(r)$ to be inferred together with the symmetric response functions.

IX. CONCLUSIONS

We have developed a continuum hydrodynamic framework for the dynamics of active force dipoles embedded in compressible supported membranes with odd (Hall) viscosity. Starting from a generalized two-dimensional Stokes equation with momentum leakage to the surrounding fluid, we derived the real-space Green tensor describing the membrane mobility using a Hankel transform solution. The resulting response tensor has the structure

$$G_{ij}(\mathbf{r}) = A_0(r) \delta_{ij} + A_1(r) \hat{r}_i \hat{r}_j + A_2(r) \varepsilon_{ij},$$

where the symmetric kernels A_0 and A_1 describe the conventional dissipative hydrodynamic response while the antisymmetric kernel A_2 encodes the chiral contribution associated with odd viscosity. The radial functions are governed by screened hydrodynamic modes determined by the interplay between membrane viscosity, compressibility, and momentum leakage into the surrounding fluid.

Using this Green tensor we obtained explicit expressions for the velocity and vorticity fields generated by an active force dipole in a compressible membrane. The dipolar flow separates naturally into longitudinal, radial, and transverse components, with the transverse component receiving contributions from the odd-viscous sector. The vorticity field likewise decomposes into even and odd parts with distinct angular structures.

Several useful limits of the theory were analyzed. In the parity-symmetric limit $\eta_o \rightarrow 0$, the antisymmetric kernel vanishes and the Green tensor reduces to the standard compressible membrane mobility with shear and compressional screening lengths. In the incompressible limit the longitudinal mode is suppressed and the flow reduces to the screened two-dimensional Stokes response. A particularly transparent regime arises in the degenerate case where the hydrodynamic screening lengths coincide, allowing compact expressions

for the Green tensor and the dipolar flow fields.

In the near field the Green tensor retains the logarithmic structure characteristic of two-dimensional hydrodynamics. The dipolar velocity decays as r^{-1} and the vorticity exhibits a quadrupolar r^{-2} structure, while odd viscosity contributes a transverse flow component and a chiral distortion of the vorticity pattern. In the far field the symmetric sector generates algebraically decaying translational interactions whereas the antisymmetric contribution is exponentially screened. As a consequence, dipole translation decays as r^{-3} while rotational couplings become exponentially small at large separations.

Building on the single-dipole solution, we formulated the dynamical equations governing interacting dipoles on the membrane. The resulting many-body system couples dipole positions and orientations through hydrodynamic interactions determined by the Green tensor kernels. The framework also yields evolution equations for global observables such as the center-of-mass motion and the polarization of the dipole ensemble. Specializing to two dipoles produces a closed nonlinear system whose near-field dynamics exhibits chiral spiral trajectories, while in the far field translational motion dominates and orientational relaxation becomes exponentially slow.

Finally, we examined how odd viscosity enters observable features of dipole pair dynamics. Quantities such as transverse pair motion and orbital rotation generally contain contributions from both symmetric and antisymmetric sectors of the Green tensor, whereas terms involving derivatives of the kernel $A_2(r)$ isolate the purely odd-viscous response. These results therefore provide a systematic framework for analyzing and interpreting odd-viscous contributions in simulations and experiments involving active inclusions in membrane systems.

The dynamical formulation developed here also provides a natural basis for studying collective phenomena in large assemblies of active dipoles. In forthcoming work [51] we will present more multidipole simulations in compressible and odd-viscous membranes based on the framework developed in this paper, exploring the emergent dynamics of interacting active inclusions in chiral membrane fluids.

X. ACKNOWLEDGMENTS

We are very thankful to Sarthak Bagaria, Michael D Graham, Naomi Oppenheimer, Haim Diamant and Mark Henle. S.K. is supported by an Institute fellowship from Birla Institute of Technology and Science, Pilani (Hyderabad Campus). R.S is supported by DST INSPIRE Faculty fellowship, India (Grant No.IFA19-PH231), NFSG and OPERA Research Grant from Birla Institute of Technology and Science, Pilani (Hyderabad Campus).

XI. DATA AVAILABILITY

The data that supports the findings of this study are available within the article.

Appendix A: Detailed Simulation Figures

Appendix B: Real-space Green's function for a compressible membrane with odd viscosity

The starting point of this section is the Fourier-space representation of the Green's tensor $G_{ij}(\mathbf{k})$ obtained by solving the linear Stokes equations (regulated by the Brinkman friction) in momentum space, as derived for two-dimensional fluid layers with odd viscosity in Refs. [47, 48]. While those works obtain real-space Green's functions in specific limiting cases, here we carry out the Fourier inversion in full generality for a compressible supported membrane with finite odd viscosity. Solving the linear Stokes-Brinkman equations for a compressible membrane with shear, dilatational, and odd viscosities in Fourier space, and eliminating the pressure using the lubrication-approximated compressibility relation, yields a closed 2×2 linear system for the longitudinal and transverse velocity modes. Inverting this system gives the mobility tensor $v_i(\mathbf{k}) = G_{ij}(\mathbf{k})F_j(\mathbf{k})$ in terms of three hydrodynamic screening lengths: the shear screening length $\kappa^{-1} = \sqrt{\eta_s/\zeta_{\parallel}}$, the compressional screening length $\lambda^{-1} = \sqrt{h(\eta_s + \eta_d)/(3\eta + h\zeta_{\parallel})}$, and the odd-viscous length $\nu^{-1} = \sqrt{\eta_o/\zeta_{\perp}}$. The resulting Green's tensor contains longitudinal, transverse, and antisymmetric components and reads

$$G_{ij}(\mathbf{k}) = \frac{\eta_s(k^2 + \kappa^2) \hat{k}_i \hat{k}_j + (\eta_s + \eta_d)(k^2 + \lambda^2) \bar{k}_i \bar{k}_j - \eta_o(k^2 + \nu^2) \varepsilon_{ij}}{D(k)}, \quad (\text{B1})$$

Incompressible membrane – Near-zone – Dynamical orientations

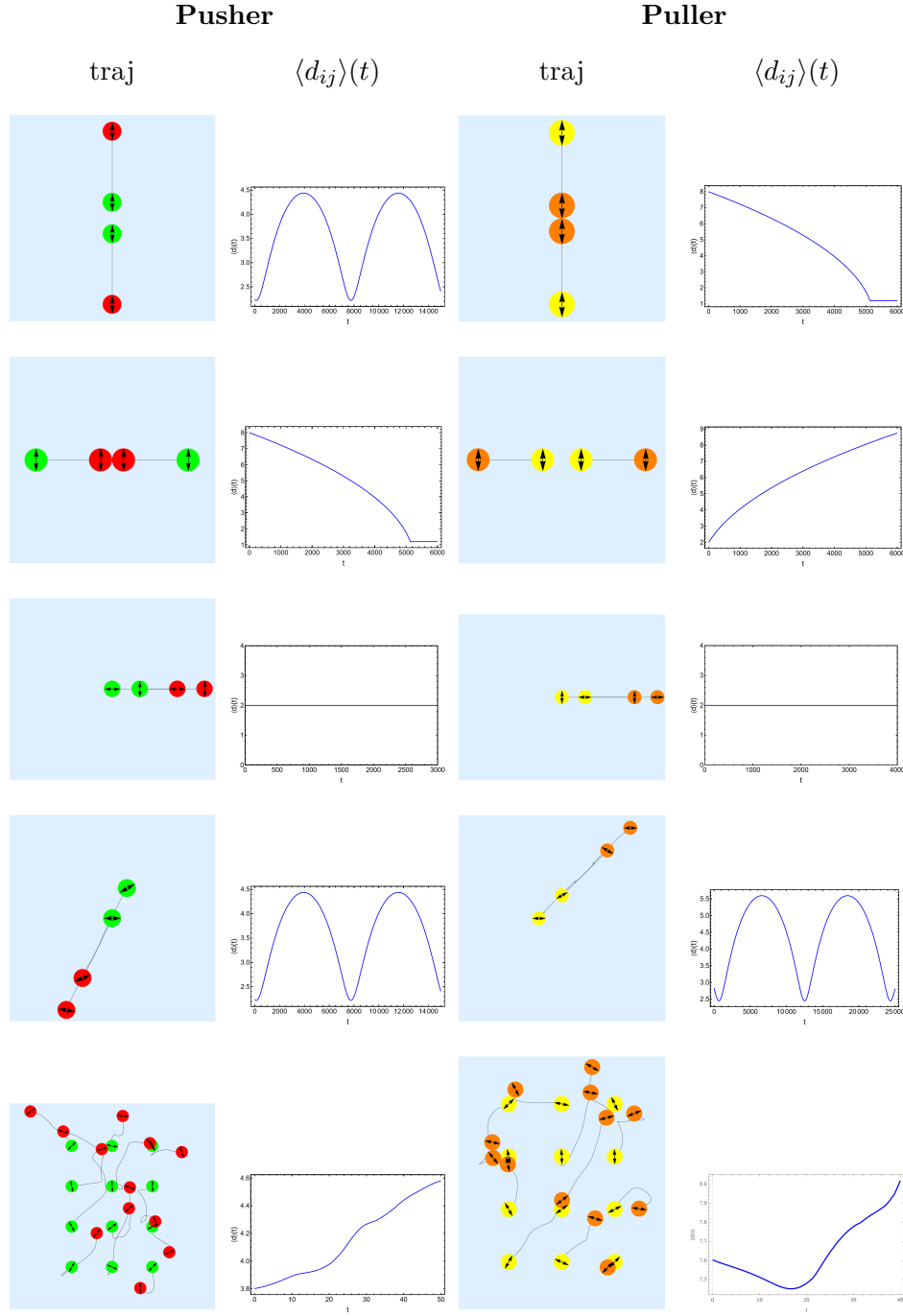


FIG. 2: Near-zone dynamics of pusher and puller motors in an incompressible supported membrane with dynamical orientations. Rows: axial, side-by-side, perpendicular, random pair, 12-dipole cluster. Columns: trajectories and mean pair separation for pusher (left) and puller (right) dipoles.

Incompressible membrane – Far-zone – Dynamical orientations

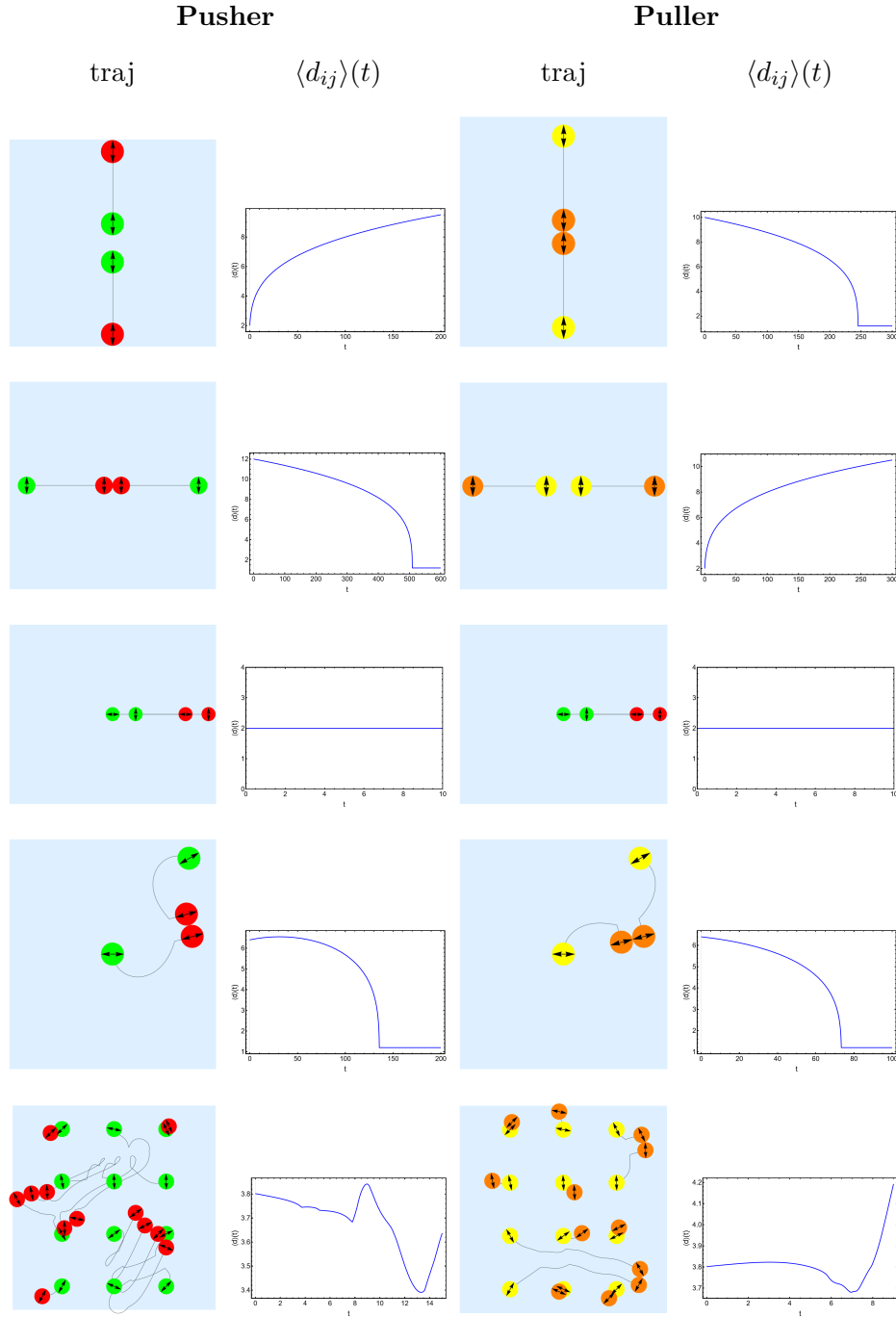


FIG. 3: Far-zone dynamics of pusher and puller dipoles in an incompressible supported membrane with *dynamical* orientations. Rows correspond to axial, side-by-side, perpendicular, random, and cluster configurations. Columns show trajectories and mean pair separations for pushers (left) and pullers (right).

Incompressible membrane – Near-zone – Quenched orientations

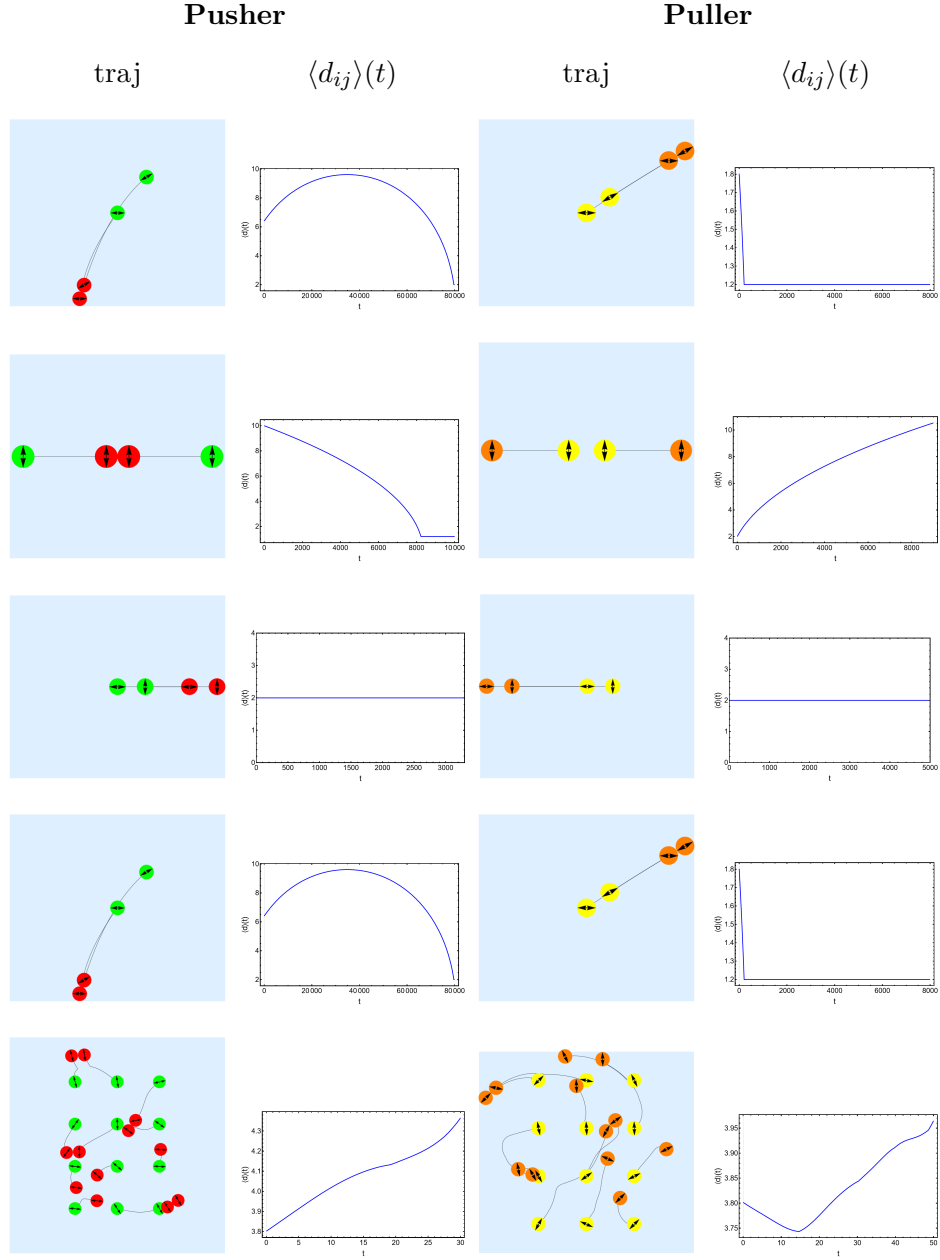


FIG. 4: Near-zone dynamics of pusher and puller dipoles in an incompressible supported membrane with *quenched* orientations. Rows correspond to axial, side-by-side, perpendicular, random, and cluster configurations. Columns show trajectories and mean separations for pushers (left) and pullers (right).

Incompressible membrane – Far-zone – Quenched orientations

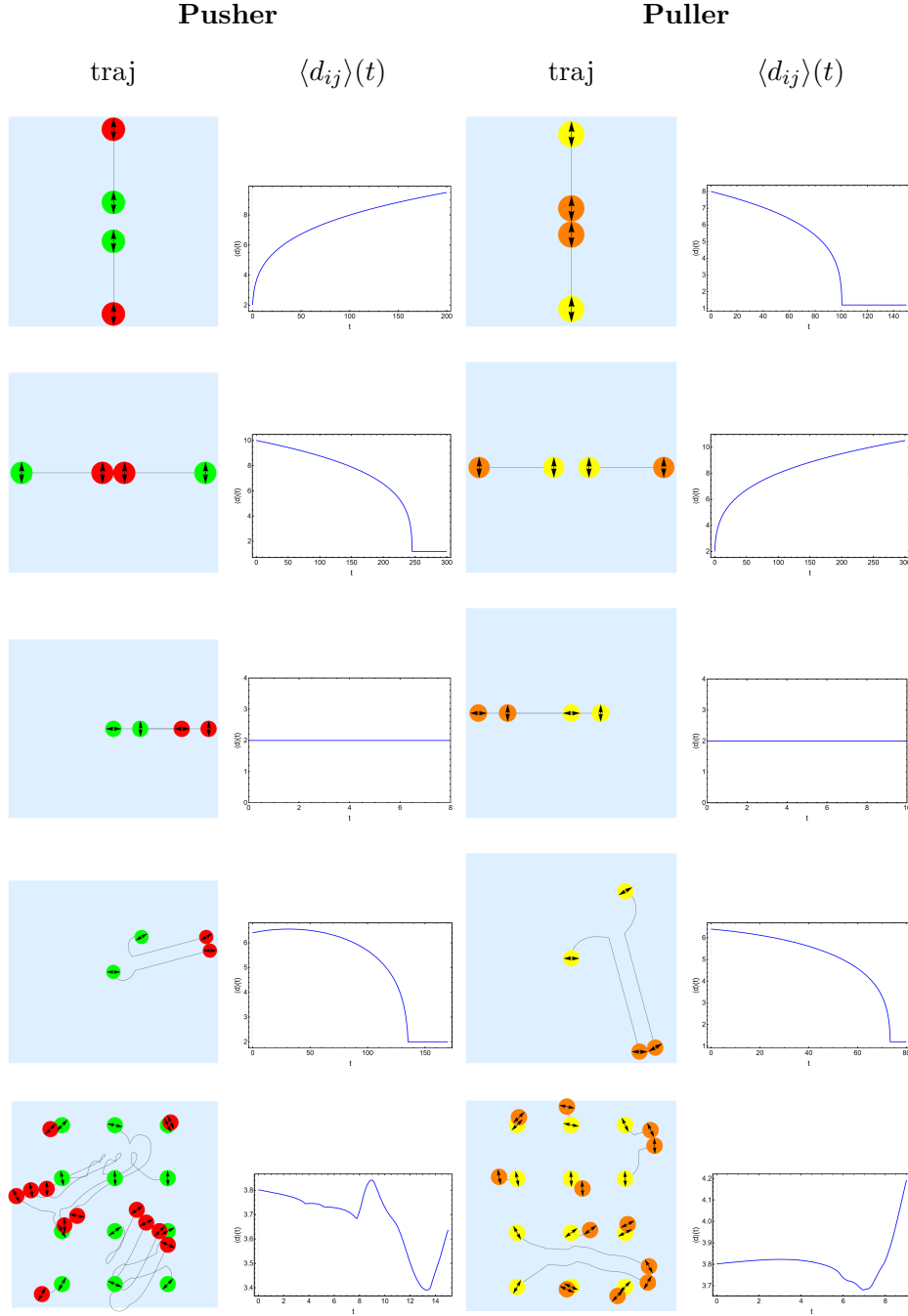


FIG. 5: Far-zone dynamics of pusher and puller dipoles in an incompressible supported membrane with *quenched* orientations. Rows correspond to axial, side-by-side, perpendicular, random, and cluster configurations. Columns show trajectories and mean separations for pushers (left) and pullers (right).

Compressible membrane (zero odd viscosity) – Near zone – Dynamical orientations

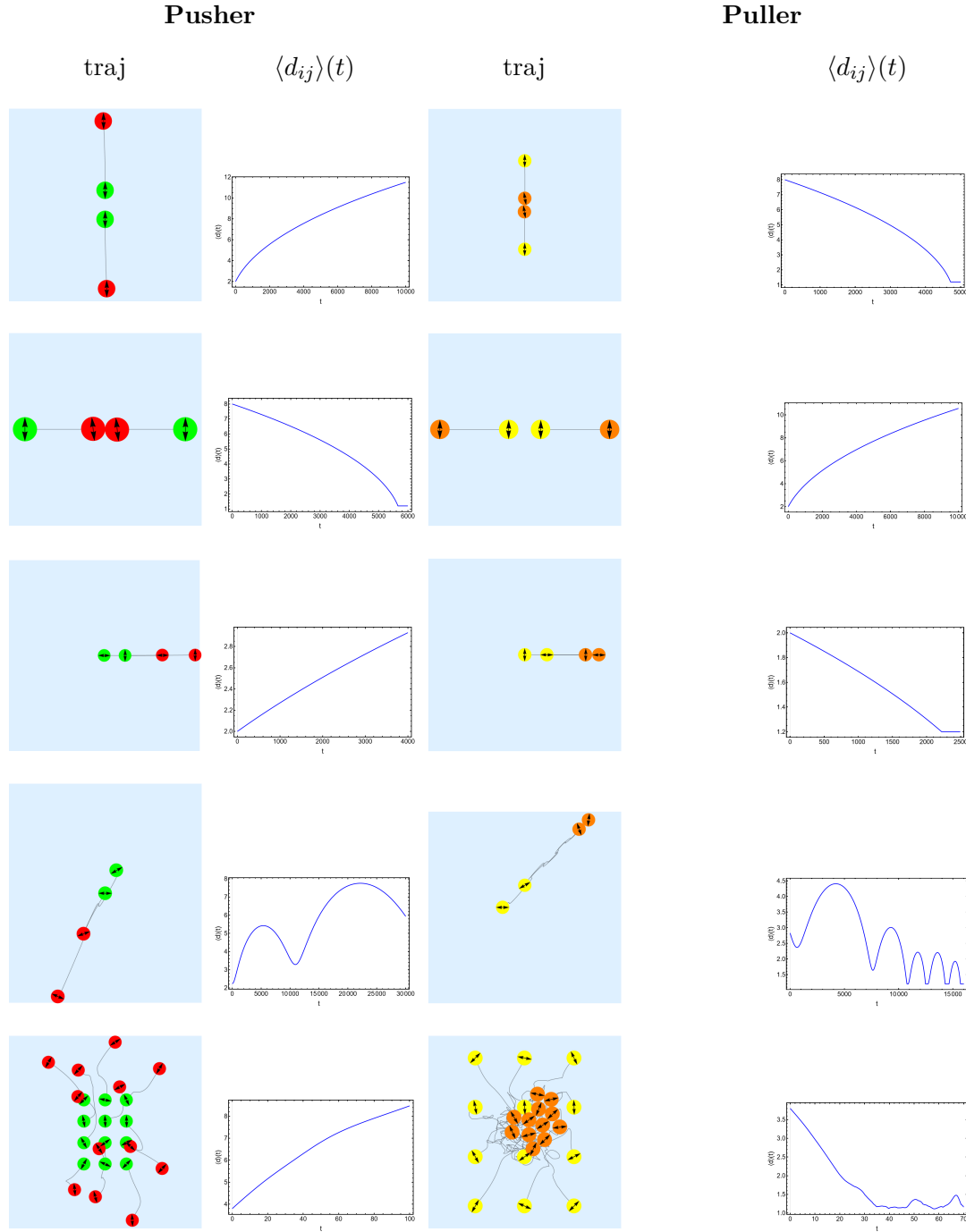


FIG. 6: Near-zone dynamics of pusher and puller dipoles in a compressible supported membrane with vanishing odd viscosity and *dynamical* orientations. Rows: axial, side-by-side, perpendicular, random pair, and 12-dipole cluster. Columns: trajectories and mean pair separation for pushers (left) and pullers (right).

Compressible membrane (zero odd viscosity) – Far zone – Dynamical orientations

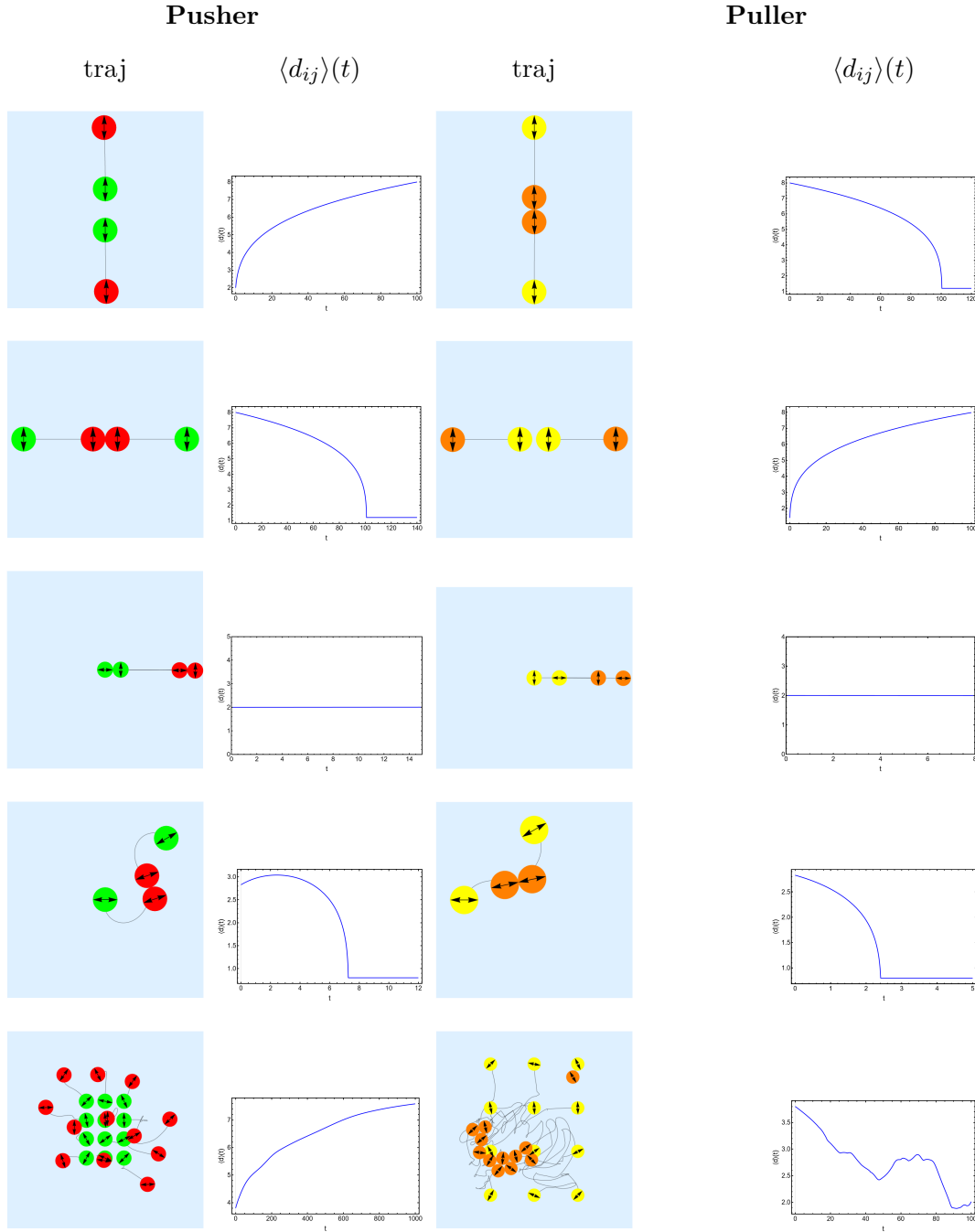


FIG. 7: Far-zone dynamics of pusher and puller dipoles in a compressible supported membrane with vanishing odd viscosity and *dynamical* orientations. Rows: axial, side-by-side, perpendicular, random pair, and 12-dipole cluster. Columns: trajectories and mean pair separation for pushers (left) and pullers (right).

Compressible membrane (zero odd viscosity) – Near zone – Quenched orientations

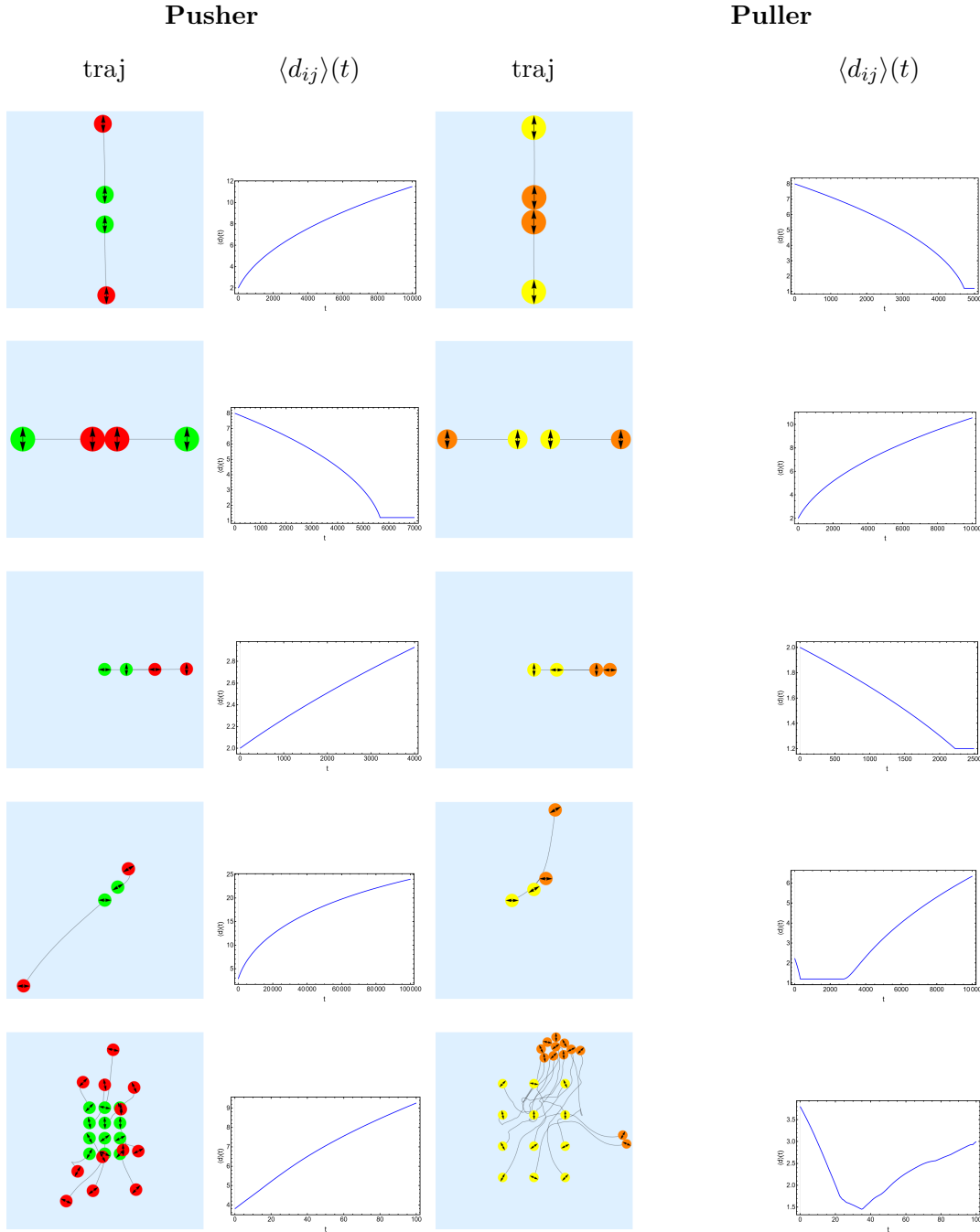


FIG. 8: Near-zone dynamics of pusher and puller dipoles in a compressible supported membrane with vanishing odd viscosity and *quenched* orientations. Rows: axial, side-by-side, perpendicular, random pair, and 12-dipole cluster. Columns: trajectories and mean pair separation for pushers (left) and pullers (right).

Compressible membrane (zero odd viscosity) – Far zone – Quenched orientations

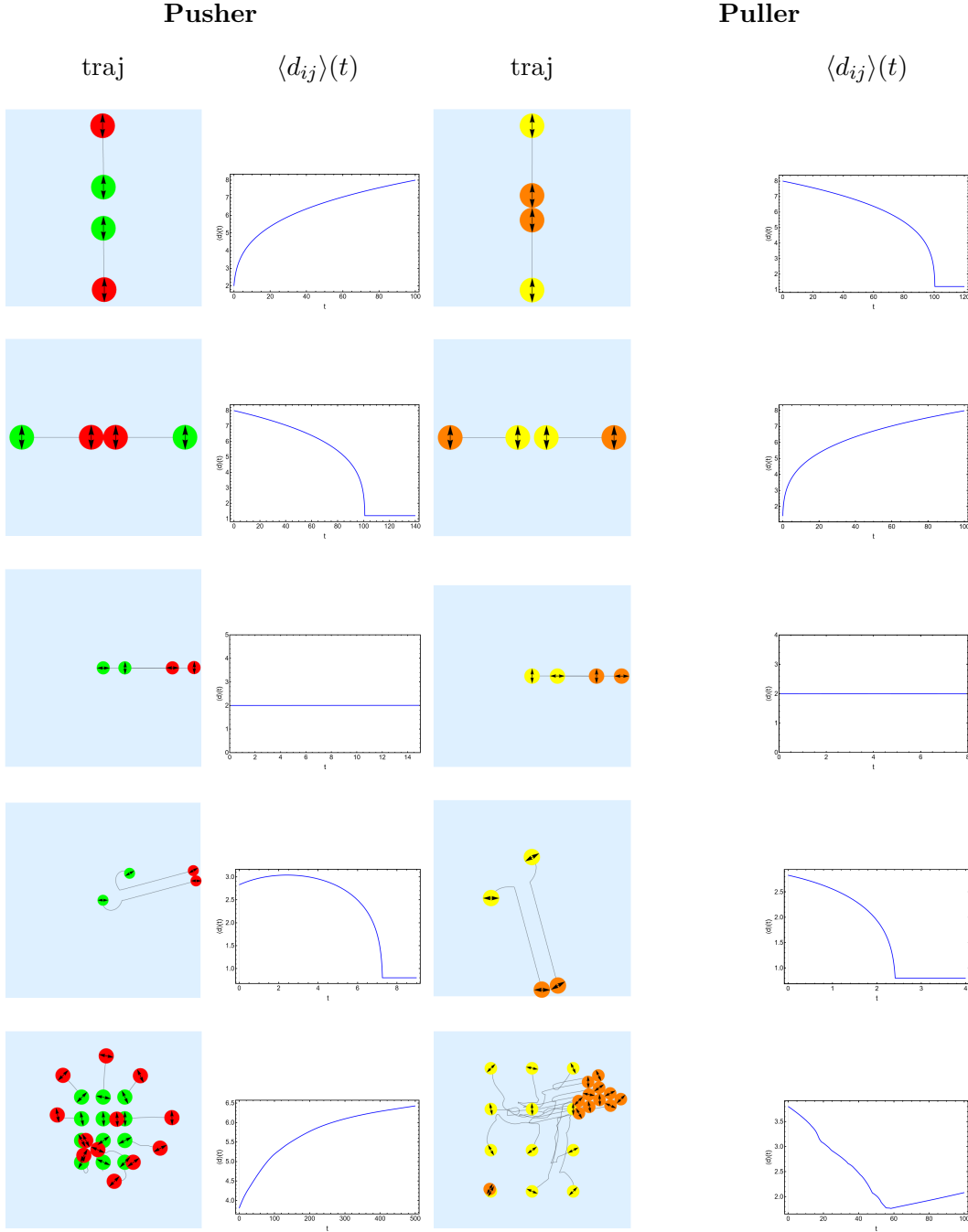


FIG. 9: Far-zone dynamics of pusher and puller dipoles in a compressible supported membrane with vanishing odd viscosity and *quenched* orientations. Rows: axial, side-by-side, perpendicular, random pair, and 12-dipole cluster. Columns: trajectories and mean pair separation for pushers (left) and pullers (right).

Compressible membrane with odd viscosity – Near zone – Dynamical orientations

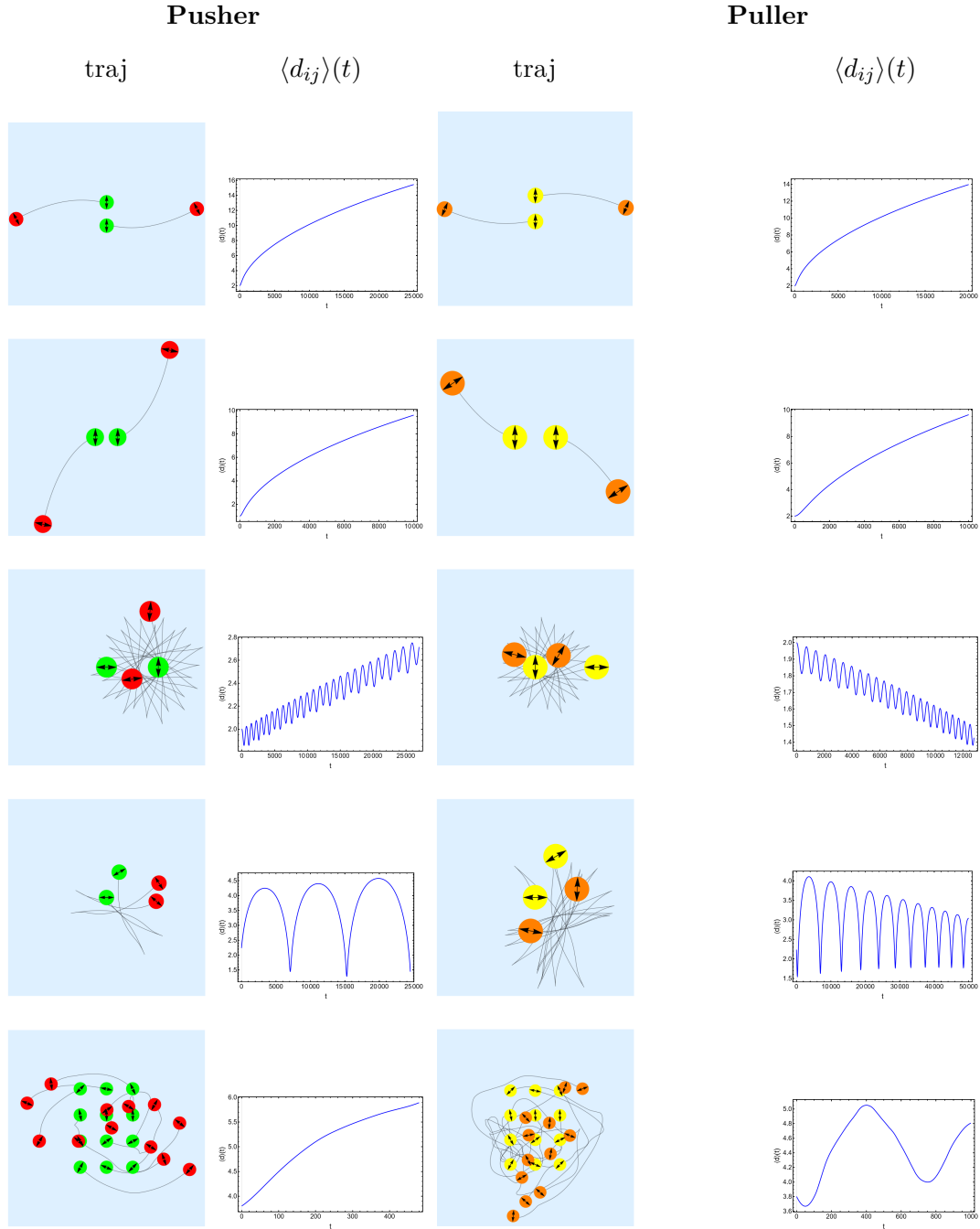


FIG. 10: Near-zone dynamics of pusher and puller dipoles in a compressible supported membrane with finite odd viscosity and *dynamical* orientations. Rows: axial, side-by-side, perpendicular, random pair, and 12-dipole cluster. Columns: trajectories and mean pair separation for pushers (left) and pullers (right).

Compressible membrane with odd viscosity – Far zone – Dynamical orientations

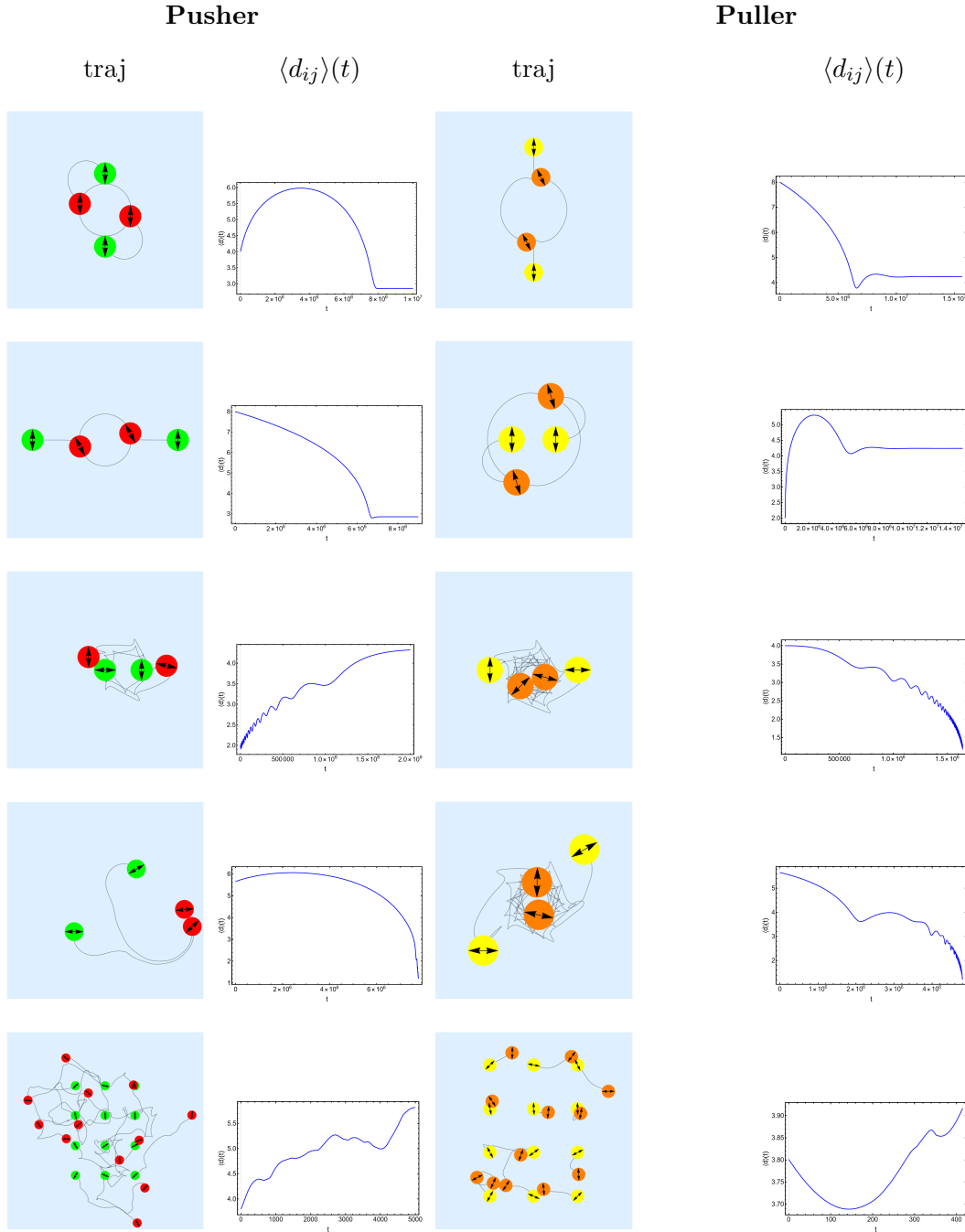


FIG. 11: Far-zone dynamics of pusher and puller dipoles in a compressible supported membrane with finite odd viscosity and *dynamical* orientations. Rows: axial, side-by-side, perpendicular, random pair, and 12-dipole cluster. Columns: trajectories and mean pair separation for pushers (left) and pullers (right).

Compressible membrane with odd viscosity – Near zone – Quenched orientations

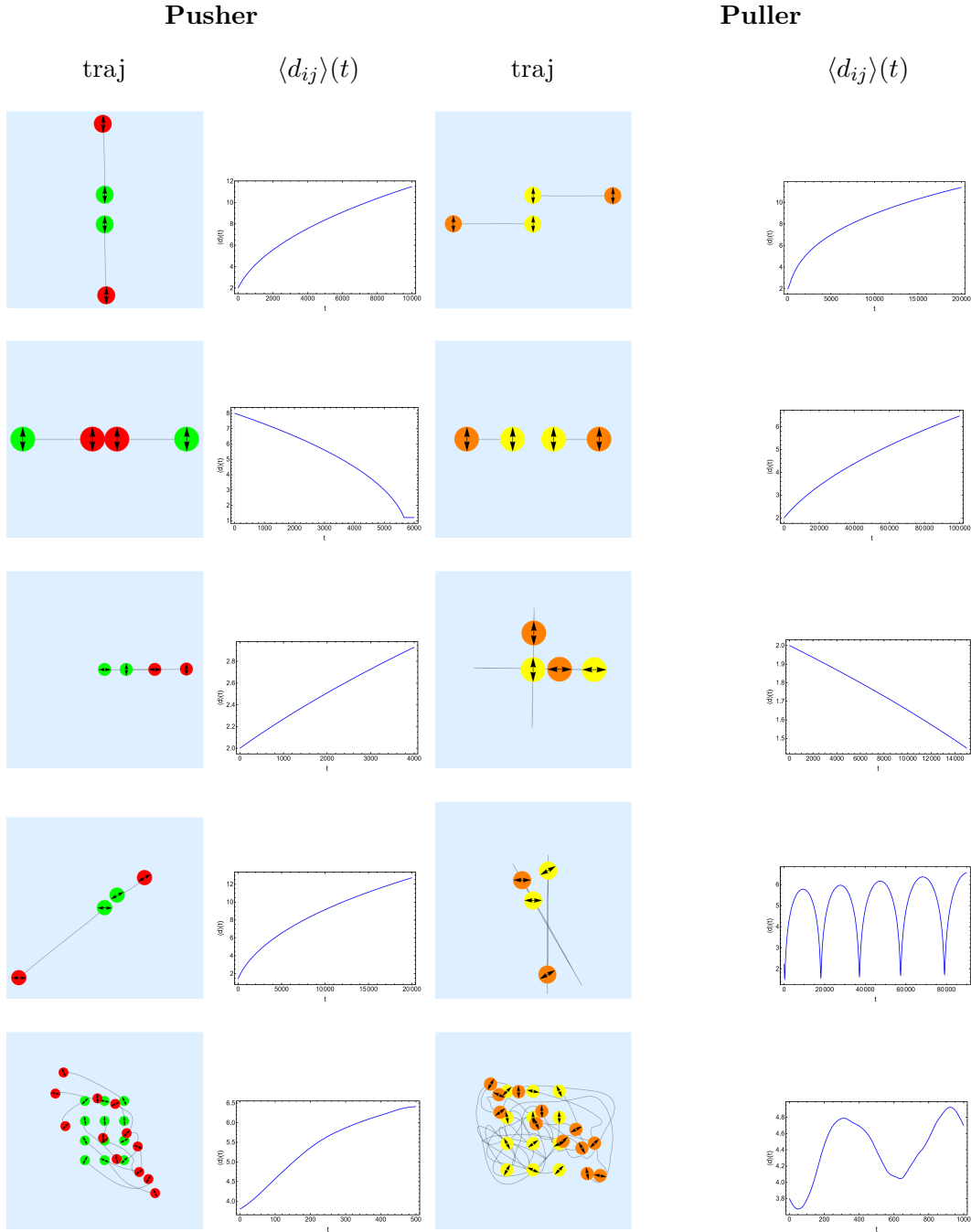


FIG. 12: Near-zone dynamics of pusher and puller dipoles in a compressible supported membrane with finite odd viscosity and *quenched* orientations. Rows: axial, side-by-side, perpendicular, random pair, and 12-dipole cluster. Columns: trajectories and mean pair separation for pushers (left) and pullers (right).

Compressible membrane with odd viscosity – Far zone – Quenched orientations

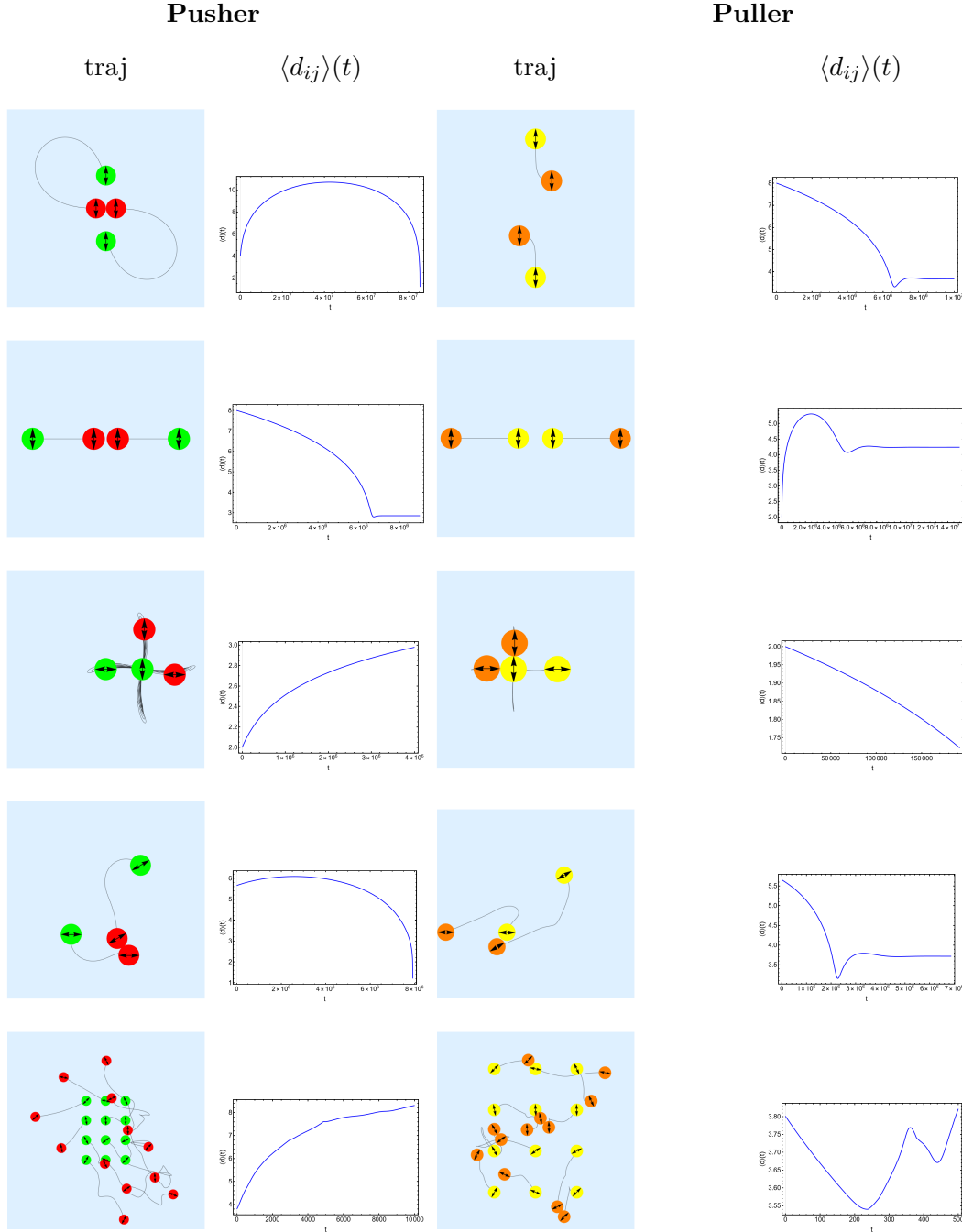


FIG. 13: Far-zone dynamics of pusher and puller dipoles in a compressible supported membrane with finite odd viscosity and *quenched* orientations. Rows: axial, side-by-side, perpendicular, random pair, and 12-dipole cluster. Columns: trajectories and mean pair separation for pushers (left) and pullers (right).

with

$$D(k) = \eta_s(\eta_s + \eta_d)(k^2 + \kappa^2)(k^2 + \lambda^2) + \eta_o^2(k^2 + \nu^2)^2.$$

Here η_s and η_d are the shear and dilatational 2D viscosities, κ^{-1} , λ^{-1} and ν^{-1} are hydrodynamic screening lengths defined in main text, and we use the unit vectors $\hat{k}_i = k_i/k$, $\bar{k}_i = -\varepsilon_{ij}\hat{k}_j$ with $\varepsilon_{12} = -\varepsilon_{21} = 1$.

The real-space tensor is defined by the inverse Fourier transform

$$G_{ij}(\mathbf{r}) = \int \frac{d^2k}{(2\pi)^2} e^{i\mathbf{k}\cdot\mathbf{r}} G_{ij}(\mathbf{k}), \quad r = |\mathbf{r}|, \quad \hat{r}_i = r_i/r.$$

By rotational invariance in the membrane plane the result will take the form

$$G_{ij}(\mathbf{r}) = A_0(r) \delta_{ij} + A_1(r) \hat{r}_i \hat{r}_j + A_2(r) \varepsilon_{ij}, \quad (\text{B2})$$

and then we proceed to obtain explicit expressions for $A_0(r)$, $A_1(r)$ and $A_2(r)$. It is convenient to decompose the Fourier-space tensor into scalar functions multiplying isotropic projectors. Using $\delta_{ij} = \hat{k}_i \hat{k}_j + \bar{k}_i \bar{k}_j$ and $\bar{k}_i \bar{k}_j = \delta_{ij} - \hat{k}_i \hat{k}_j$, the tensor (B1) can be rewritten as

$$G_{ij}(\mathbf{k}) = \beta(k) \delta_{ij} + [\alpha(k) - \beta(k)] \hat{k}_i \hat{k}_j + \gamma(k) \varepsilon_{ij}, \quad (\text{B3})$$

where

$$\alpha(k) = \frac{\eta_s(k^2 + \kappa^2)}{D(k)}, \quad \beta(k) = \frac{(\eta_s + \eta_d)(k^2 + \lambda^2)}{D(k)}, \quad \gamma(k) = -\frac{\eta_o(k^2 + \nu^2)}{D(k)}.$$

Since all scalar functions depend only on $k = |\mathbf{k}|$, we can use polar coordinates (k, θ) with $\mathbf{k} \cdot \mathbf{r} = kr \cos \theta$ and the identity $\int_0^{2\pi} d\theta e^{ikr \cos \theta} = 2\pi J_0(kr)$ to reduce the inverse transform to Hankel transforms. For any isotropic scalar $F(k)$ we define the Hankel transform

$$\mathcal{H}\{F\}(r) = \int_0^\infty \frac{k dk}{2\pi} F(k) J_0(kr). \quad (\text{B4})$$

Standard Fourier identities then give

$$G_{ij}(\mathbf{r}) = \delta_{ij} \Psi(r) - \partial_i \partial_j \Phi(r) + \varepsilon_{ij} \chi(r), \quad (\text{B5})$$

with

$$\Psi(r) = \mathcal{H}\{\beta\}(r), \quad \chi(r) = \mathcal{H}\{\gamma\}(r),$$

and

$$\Phi(r) = \int_0^\infty \frac{k dk}{2\pi} \frac{\alpha(k) - \beta(k)}{k^2} J_0(kr). \quad (\text{B6})$$

For a purely radial scalar $\Phi(r)$ we have

$$\partial_i \Phi = \Phi'(r) \hat{r}_i, \quad \partial_i \partial_j \Phi = \hat{r}_i \hat{r}_j \Phi''(r) + (\delta_{ij} - \hat{r}_i \hat{r}_j) \frac{\Phi'(r)}{r}. \quad (\text{B7})$$

Substituting (B7) into (B5) and comparing with the form (B2) yields

$$A_0(r) = \Psi(r) - \frac{\Phi'(r)}{r}, \quad A_1(r) = -\Phi''(r) + \frac{\Phi'(r)}{r}, \quad A_2(r) = \chi(r). \quad (\text{B8})$$

The remainder of the derivation is therefore the evaluation of $\Psi(r)$, $\chi(r)$, and $\Phi(r)$. Introducing the variable $s = k^2$, so that $D(k) \equiv D(s)$ is a quadratic polynomial,

$$D(s) = As^2 + Bs + C, \quad (\text{B9})$$

with coefficients

$$A = \eta_s(\eta_s + \eta_d) + \eta_o^2, \quad B = \eta_s(\eta_s + \eta_d)(\kappa^2 + \lambda^2) + 2\eta_o^2\nu^2, \quad C = \eta_s(\eta_s + \eta_d)\kappa^2\lambda^2 + \eta_o^2\nu^4.$$

Let s_1 and s_2 be the roots of $D(s)$,

$$D(s) = A(s - s_1)(s - s_2), \quad s_{1,2} = \frac{-B \pm \sqrt{\Delta}}{2A}, \quad \Delta = B^2 - 4AC, \quad (\text{B10})$$

and let us also define the positive screening masses

$$m_i = \sqrt{-s_i}, \quad i = 1, 2.$$

Each of the scalar functions in (B4) is a rational function of s with denominator $D(s)$ and a linear numerator; therefore it admits a partial-fraction representation. For the isotropic sector β and the antisymmetric sector γ we write

$$\beta(s) = \frac{(\eta_s + \eta_d)(s + \lambda^2)}{D(s)} = \sum_{i=1}^2 \frac{R_i^{(\beta)}}{s - s_i}, \quad \gamma(s) = -\frac{\eta_o(s + \nu^2)}{D(s)} = \sum_{i=1}^2 \frac{R_i^{(\gamma)}}{s - s_i}, \quad (\text{B11})$$

with residues

$$R_i^{(\beta)} = \frac{(\eta_s + \eta_d)(s_i + \lambda^2)}{A(s_i - s_j)}, \quad R_i^{(\gamma)} = -\frac{\eta_o(s_i + \nu^2)}{A(s_i - s_j)}, \quad i \neq j.$$

For the longitudinal sector we consider

$$\frac{\alpha(s) - \beta(s)}{s} = \frac{N_\Phi(s)}{sD(s)}, \quad (\text{B12})$$

where

$$N_\Phi(s) = \eta_s(s + \kappa^2) - (\eta_s + \eta_d)(s + \lambda^2) = -\eta_d s + [\eta_s \kappa^2 - (\eta_s + \eta_d) \lambda^2].$$

We decompose this as

$$\frac{N_{\Phi}(s)}{sD(s)} = \frac{C_0}{s} + \frac{C_1}{s-s_1} + \frac{C_2}{s-s_2}, \quad (\text{B13})$$

with

$$C_0 = \frac{N_{\Phi}(0)}{D(0)} = \frac{\eta_s \kappa^2 - (\eta_s + \eta_d) \lambda^2}{C},$$

and

$$C_i = \frac{N_{\Phi}(s_i)}{s_i D'(s_i)} = \frac{-\eta_d s_i + [\eta_s \kappa^2 - (\eta_s + \eta_d) \lambda^2]}{s_i A(s_i - s_j)}, \quad i \neq j.$$

The Hankel transform (B4) of each simple pole is given by the standard identity

$$\int_0^{\infty} \frac{k dk}{2\pi} \frac{J_0(kr)}{k^2 + m^2} = \frac{1}{2\pi} K_0(mr), \quad (\text{B14})$$

where K_ν is the modified Bessel function of the second kind. A logarithmic kernel arises from the $1/s$ term in (B13),

$$\int_0^{\infty} \frac{k dk}{2\pi} \frac{J_0(kr)}{k^2} = \frac{1}{2\pi} (C_{\text{reg}} - \ln r),$$

where C_{reg} is a regularization constant that drops out of the final expressions after differentiation. Using the so-constructed partial-fraction forms we thus obtain

$$\Psi(r) = \mathcal{H}\{\beta\}(r) = \frac{1}{2\pi} \sum_{i=1}^2 R_i^{(\beta)} K_0(m_i r), \quad (\text{B15})$$

$$\chi(r) = \mathcal{H}\{\gamma\}(r) = \frac{1}{2\pi} \sum_{i=1}^2 R_i^{(\gamma)} K_0(m_i r), \quad (\text{B16})$$

$$\begin{aligned} \Phi(r) &= \int_0^{\infty} \frac{k dk}{2\pi} \frac{\alpha(k) - \beta(k)}{k^2} J_0(kr) \\ &= -\frac{C_0}{2\pi} \ln r + \frac{1}{2\pi} \sum_{i=1}^2 C_i K_0(m_i r) + \text{const.} \end{aligned} \quad (\text{B17})$$

We differentiate (and use another standard identity $K_0'(x) = -K_1(x)$) to obtain

$$\Phi'(r) = -\frac{C_0}{2\pi} \frac{1}{r} - \frac{1}{2\pi} \sum_{i=1}^2 C_i m_i K_1(m_i r), \quad (\text{B18})$$

$$\Phi''(r) = \frac{C_0}{2\pi} \frac{1}{r^2} + \frac{1}{2\pi} \sum_{i=1}^2 C_i \left[m_i^2 K_0(m_i r) + \frac{m_i}{r} K_1(m_i r) \right]. \quad (\text{B19})$$

Substituting Eqs. (B17)–(B19) into Eqs. (B8) yields the explicit coefficients in Eq. (B2):

$$A_0(r) = \frac{1}{2\pi} \sum_{i=1}^2 R_i^{(\beta)} K_0(m_i r) + \frac{C_0}{2\pi} \frac{1}{r^2} + \frac{1}{2\pi} \sum_{i=1}^2 C_i \frac{m_i}{r} K_1(m_i r), \quad (\text{B20})$$

$$A_1(r) = -\frac{1}{2\pi} \sum_{i=1}^2 C_i m_i^2 K_0(m_i r) - \frac{1}{\pi} \sum_{i=1}^2 C_i \frac{m_i}{r} K_1(m_i r) - \frac{C_0}{\pi} \frac{1}{r^2}, \quad (\text{B21})$$

$$A_2(r) = \frac{1}{2\pi} \sum_{i=1}^2 R_i^{(\gamma)} K_0(m_i r), \quad (\text{B22})$$

with the coefficients A, B, C , the roots s_i , the masses m_i , and the residues $R_i^{(\beta)}$, $R_i^{(\gamma)}$, C_0 , C_i defined in Eqs. (B10), (B12), (B14), and (B14). These expressions coincide with the real-space Green's function quoted in Eqs. (6)–(7) of the main text.

1. Structure of the pole contributions

The spatial structure of the membrane response is governed by the poles $m_{1,2}$ of the generalized Stokes operator,

$$m_{1,2}^2 = \frac{B \mp \sqrt{\Delta}}{2A}, \quad \Delta = B^2 - 4AC.$$

After eliminating ν using $\nu^2 = \zeta_{\perp}/\eta_o$, and treating ζ_{\perp} as fixed, the coefficients become

$$A = S + \eta_o^2, \quad B = S(\kappa^2 + \lambda^2) + 2\zeta_{\perp}\eta_o, \quad C = S\kappa^2\lambda^2 + \zeta_{\perp}^2,$$

where $S = \eta_s(\eta_s + \eta_d)$. The discriminant then takes the form

$$\Delta = S^2(\kappa^2 - \lambda^2)^2 + 4S(\kappa^2 + \lambda^2)\zeta_{\perp}\eta_o - 4S\zeta_{\perp}^2 - 4S\kappa^2\lambda^2\eta_o^2.$$

Since the coefficient of η_o^2 is negative, $\Delta(\eta_o)$ is a downward-opening parabola. Solving $\Delta = 0$ gives the two critical values

$$\eta_{o,\pm} = \frac{\zeta_{\perp}(\kappa^2 + \lambda^2) \pm |\kappa^2 - \lambda^2| \sqrt{\zeta_{\perp}^2 + \kappa^2\eta_s(\eta_s + \eta_d)\lambda^2}}{2\kappa^2\lambda^2}.$$

Hence $\Delta > 0$ for $\eta_{o,-} < \eta_o < \eta_{o,+}$, and the poles $m_{1,2}$ are real. In this regime the membrane response is a superposition of two purely exponentially screened hydrodynamic modes. Outside this interval, $\Delta < 0$ and the poles form a complex-conjugate pair $m_{1,2} = a \pm ib$.

For the positive-parameter branch considered here one has $A > 0$ and $B > 0$, so the complex poles lie in the right half-plane on the principal branch and therefore have positive real part. The response thus remains exponentially screened while acquiring an oscillatory component. The pole contribution to the Green tensor then behaves asymptotically as

$$G_{ij}^{\text{pole}}(r) \sim \frac{e^{-ar}}{\sqrt{r}} \cos(br - \phi),$$

up to tensorial prefactors. When the algebraic coefficient C_0 in the general real-space Green tensor is nonzero, this oscillatory screened contribution is accompanied by the algebraic $1/r^2$ term already present in the full solution.

The three possibilities $\Delta > 0$, $\Delta = 0$, and $\Delta < 0$ therefore correspond respectively to overdamped-like, critically damped, and underdamped-like screened hydrodynamic response.

These general results simplify in several useful limits.

In the compressible parity-symmetric limit $\eta_o \rightarrow 0$, the discriminant reduces to

$$\Delta = [\eta_s(\eta_s + \eta_d)]^2(\kappa^2 - \lambda^2)^2 \geq 0,$$

so the poles are always real. The screening masses reduce to

$$m_1^2 = \lambda^2, \quad m_2^2 = \kappa^2,$$

up to relabeling. The hydrodynamic response therefore decomposes into independent compressional and shear screening channels.

In the incompressible parity-symmetric limit $\eta_o \rightarrow 0$, $\eta_d \rightarrow \infty$, the longitudinal screening scale diverges and formally

$$m_1^2 = 0, \quad m_2^2 = \kappa^2.$$

In this limit the longitudinal sector decouples and its residue vanishes, so the only nontrivial hydrodynamic screening that remains is the transverse shear mode with screening length κ^{-1} .

Finally, in the identical-screening degenerate limit $\kappa = \lambda = \nu = m$, together with $\eta_d = 3\eta_s$ and $\zeta_{\perp} = (\eta_o/\eta_s)\zeta_{\parallel}$, the discriminant vanishes,

$$\Delta = 0, \quad m_1 = m_2 = m.$$

The two poles therefore coalesce into a repeated screening mass and the Green tensor becomes controlled by a single length scale $\ell = m^{-1}$. This limit realizes the coalescence condition $\Delta = 0$ on a special constrained submanifold of parameter space. In this regime odd viscosity no longer shifts the pole locations, but instead modifies the residues and generates the antisymmetric component of the Green tensor.

Appendix C: Parity structure of the Green tensor

The parity properties of the Green tensor follow directly from the symmetry of the governing hydrodynamic equations. Consider a reflection in the membrane plane described by a matrix P satisfying $P^2 = I$ and $\det P = -1$. Under this transformation

$$r'_i = P_{ij}r_j, \quad v'_i(\mathbf{r}') = P_{ij}v_j(\mathbf{r}). \quad (\text{C1})$$

The isotropic tensor is invariant,

$$P\delta P^T = \delta, \quad (\text{C2})$$

whereas the antisymmetric tensor changes sign,

$$P\varepsilon P^T = -\varepsilon. \quad (\text{C3})$$

Consequently the terms proportional to ε_{ij} in the hydrodynamic operator change sign under reflection. The hydrodynamic equations are therefore mapped to those of a medium with opposite handedness. Introducing a chirality label $\chi = \pm 1$, the Green tensor satisfies the covariance relation

$$G^{(-\chi)}(\mathbf{r}') = P G^{(\chi)}(\mathbf{r}) P^T, \quad \mathbf{r}' = P\mathbf{r}. \quad (\text{C4})$$

Rotational isotropy restricts the Green tensor to the form

$$G_{ij}^{(\chi)}(\mathbf{r}) = A_0(r; \chi) \delta_{ij} + A_1(r; \chi) \hat{r}_i \hat{r}_j + A_2(r; \chi) \varepsilon_{ij}, \quad r = |\mathbf{r}|. \quad (\text{C5})$$

Substituting this decomposition into Eq. (C4) and using

$$P(\hat{r}\hat{r})P^T = \widehat{P\mathbf{r}}\widehat{P\mathbf{r}}, \quad P\varepsilon P^T = -\varepsilon, \quad (\text{C6})$$

immediately gives

$$A_0(r; \chi) = A_0(r; -\chi), \quad A_1(r; \chi) = A_1(r; -\chi), \quad A_2(r; \chi) = -A_2(r; -\chi). \quad (\text{C7})$$

Thus the coefficients multiplying the symmetric tensors δ_{ij} and $\hat{r}_i\hat{r}_j$ are even under chirality reversal, while the coefficient multiplying the antisymmetric tensor ε_{ij} is odd. This result follows purely from symmetry and does not depend on the detailed analytic form of the Green tensor.

-
- [1] E. M. Purcell, *Life at low Reynolds number*, Am. J. Phys. **45**, 3 (1977).
 - [2] E. Lauga and T. R. Powers, *The hydrodynamics of swimming microorganisms*, Rep. Prog. Phys. **72**, 096601 (2009).
 - [3] N. S. Gov and S. A. Safran, *Red blood cell membrane fluctuations and shape controlled by ATP-induced cytoskeletal defects*, Biophys. J. **88**, 1859 (2005).
 - [4] B. A. Camley and F. L. H. Brown, *Diffusion of complex objects embedded in free and supported lipid bilayer membranes: role of shape and hydrodynamic coupling*, Soft Matter **9**, 4767 (2013).
 - [5] A. S. Mikhailov and R. Kapral, *Hydrodynamic collective effects of active protein machines in solution and lipid bilayers*, Proc. Natl. Acad. Sci. USA **112**, E3639 (2015).
 - [6] O. Campàs, C. Leduc, P. Bassereau, J. Casademunt, J.-F. Joanny and J. Prost, *Coordination of kinesin motors pulling on fluid membranes*, Biophys. J. **94**, 5009 (2008).
 - [7] R. Grover, J. Fischer, F. W. Schwarz, W. J. Walter, P. Schwille and S. Diez, *Transport efficiency of membrane-anchored kinesin motors depends on motor density and diffusivity*, Proc. Natl. Acad. Sci. USA **113**, E7185 (2016).
 - [8] R. A. Simha and S. Ramaswamy, “Hydrodynamic fluctuations and instabilities in ordered suspensions of self-propelled particles,” Phys. Rev. Lett. **89**, 058101 (2002).
 - [9] D. Saintillan and M. J. Shelley, “Instabilities and pattern formation in active particle suspensions: Kinetic theory and continuum simulations,” Phys. Rev. Lett. **100**, 178103 (2008).
 - [10] D. Saintillan and M. J. Shelley, “Instabilities, pattern formation, and mixing in active suspensions,” Phys. Fluids **20**, 123304 (2008).
 - [11] S. Ramaswamy, “The mechanics and statistics of active matter,” Annu. Rev. Condens. Matter Phys. **1**, 323–345 (2010).
 - [12] M. C. Marchetti, J.-F. Joanny, S. Ramaswamy, T. B. Liverpool, J. Prost, M. Rao, and R. A. Simha, “Hydrodynamics of soft active matter,” Rev. Mod. Phys. **85**, 1143–1189 (2013).
 - [13] D. L. Koch and G. Subramanian, “Collective hydrodynamics of swimming microorganisms:

- Living fluids,” *Annu. Rev. Fluid Mech.* **43**, 637–659 (2011).
- [14] D. Saintillan, “Rheology of active fluids,” *Annu. Rev. Fluid Mech.* **50**, 563–592 (2018).
- [15] A. Baskaran and M. C. Marchetti, “Statistical mechanics and hydrodynamics of bacterial suspensions,” *Proc. Natl. Acad. Sci. USA* **106**, 15567–15572 (2009).
- [16] A. Baskaran and M. C. Marchetti, “Nonequilibrium statistical mechanics of self-propelled hard rods,” *J. Stat. Mech.* P04019 (2010).
- [17] T. Ishikawa and T. J. Pedley, “Coherent structures in monolayers of swimming particles,” *Phys. Rev. Lett.* **100**, 088103 (2008).
- [18] F. Alarcón and I. Pagonabarraga, “Spontaneous aggregation and global polar order in squirmer suspensions,” *J. Mol. Liq.* **185**, 56–61 (2013).
- [19] M. Theers, E. Westphal, K. Qi, R. G. Winkler, and G. Gompper, “Clustering of microswimmers: Interplay of shape and hydrodynamics,” *Soft Matter* **14**, 8590–8603 (2018).
- [20] A. Zöttl and H. Stark, “Emergent behavior in active colloids,” *J. Phys.: Condens. Matter* **28**, 253001 (2016).
- [21] P. G. Saffman, *Brownian motion in thin sheets of viscous fluid*, *J. Fluid Mech.* **73**, 593 (1975).
- [22] P. G. Saffman and M. Delbrück, *Brownian motion in biological membranes*, *Proc. Natl. Acad. Sci. USA* **72**, 3111 (1975).
- [23] B. D. Hughes, B. A. Pailthorpe and L. R. White, *The translational and rotational drag on a cylinder moving in a membrane*, *J. Fluid Mech.* **110**, 349 (1981).
- [24] E. Evans and E. Sackmann, *Translational and rotational drag coefficients for a disk in a supported liquid membrane*, *J. Fluid Mech.* **194**, 553 (1988).
- [25] D. K. Lubensky and R. E. Goldstein, *Hydrodynamics of monolayer domains at the air–water interface*, *Phys. Fluids* **8**, 843 (1996).
- [26] H. A. Stone and A. Ajdari, *Hydrodynamics of particles embedded in a surfactant layer over a subphase of finite depth*, *J. Fluid Mech.* **369**, 151 (1998).
- [27] T. M. Fischer, *The drag on needles moving in a Langmuir monolayer*, *J. Fluid Mech.* **498**, 123 (2004).
- [28] A. J. Levine, T. B. Liverpool, and F. C. MacKintosh, *Dynamics of rigid and flexible extended bodies in viscous films and membranes*, *Phys. Rev. Lett.* **93**, 038102 (2004).
- [29] N. Oppenheimer and H. Diamant, *Correlated diffusion of membrane proteins and their effect on membrane viscosity*, *Biophys. J.* **96**, 3041–3049 (2009).

- [30] N. Oppenheimer and H. Diamant, *Correlated dynamics of inclusions in a supported membrane*, Phys. Rev. E **82**, 041912 (2010).
- [31] N. Oppenheimer and H. Diamant, *Dynamics of membranes with immobile inclusions*, Phys. Rev. Lett. **107**, 258102 (2011).
- [32] H. Manikantan, *Tunable collective dynamics of active inclusions in viscous membranes*, Phys. Rev. Lett. **125**, 268101 (2020).
- [33] R. Samanta and N. Oppenheimer, *Vortex flows and streamline topology in curved biological membranes*, Phys. Fluids **33**, 051906 (2021).
- [34] S. Bagaria and R. Samanta, *Dynamics of force dipoles in curved fluid membranes*, Phys. Rev. Fluids **7**, 093101 (2022).
- [35] S. Jain and R. Samanta, *Force dipole interactions in tubular fluid membranes*, Phys. Fluids **35**, 071901 (2023).
- [36] U. Maurya, S. T. Gavva, A. Saha, and R. Samanta, *Vortex dynamics in tubular fluid membranes*, Phys. Fluids **37**, 073109 (2025).
- [37] S. Krishnan and R. Samanta, *Hamiltonian Active Matter in Incompressible Fluid Membranes*, arXiv:2512.03609 [cond-mat.soft] (2025).
- [38] M. Leoni and T. B. Liverpool, *Swimmers in thin films: from swarming to hydrodynamic instabilities*, Phys. Rev. Lett. **105**, 238102 (2010).
- [39] Y. Hatwalne, S. Ramaswamy, M. Rao, and R. A. Simha, *Rheology of active-particle suspensions*, Phys. Rev. Lett. **92**, 118101 (2004).
- [40] T. Vicsek, A. Czirók, E. Ben-Jacob, I. Cohen, and O. Shochet, *Novel type of phase transition in a system of self-driven particles*, Phys. Rev. Lett. **75**, 1226 (1995).
- [41] J. E. Avron, *Odd viscosity*, Phys. Rev. Lett. **80**, 2635 (1998).
- [42] D. Banerjee, A. Souslov, A. G. Abanov and V. Vitelli, *Odd viscosity in chiral active fluids*, Nat. Commun. **8**, 1573 (2017).
- [43] V. Soni, E. S. Bililign, S. Magkiriadou, S. Sacanna, D. Bartolo, M. J. Shelley, and W. T. M. Irvine, “The odd free surface flows of a colloidal chiral fluid,” Nat. Phys. **15**, 1188–1194 (2019).
- [44] S. C. Al-Izzi, B. Materassi, A. Souslov and V. Vitelli, *Chiral active membranes: odd mechanics, spontaneous flows and shape control*, Phys. Rev. Res. **5**, 043227 (2023).
- [45] C. Barentin, C. Ybert, J.-M. di Meglio, and J.-F. Joanny, “Surface shear viscosity of Gibbs

- and Langmuir monolayers,” *J. Fluid Mech.* **397**, 331 (1999).
- [46] H. Manikantan and T. M. Squires, “Surfactant dynamics: hidden variables controlling fluid flows,” *J. Fluid Mech.* **892**, P1 (2020).
- [47] Y. Hosaka, D. Andelman, and S. Komura, “Pair dynamics of active force dipoles in an odd-viscous fluid,” *Eur. Phys. J. E* **46**, 18 (2023).
- [48] Y. Hosaka, S. Komura, and D. Andelman, “Nonreciprocal response of a two-dimensional fluid with odd viscosity,” *Phys. Rev. E* **103**, 042610 (2021).
- [49] Y. Shoham and N. Oppenheimer, *Hamiltonian dynamics and structural states of two-dimensional active particles*, *Phys. Rev. Lett.* **131**, 178301 (2023).
- [50] A. Daddi-Moussa-Ider, Y. Hosaka and S. Komura, *Exact response functions for a compressible thin fluid layer with odd viscosity*, arXiv:2602.18136 (2026).
- [51] S. Krishnan, U. Maurya and R. Samanta, *Numerical Simulations of Force Dipoles in Membranes with Odd Viscosity*, manuscript in preparation (2026).